SAVONIA

THESIS – DEGREE PROGRAM IN ENVIRONMENTAL TECHNOLOGY
SAVONIA UNIVERSITY OF APPLIED SCIENCES

FURTHER DEVELOPMENT OF A CENTRIFUGAL SOLIDS SEPARATOR PROTOTYPE

Author: Priscila Gandhi Estrada Reynoso

SAVONIA UNIVERSITY OF APPLIED SCIENCES THESIS
Abstract

Field of Study Technology, Communication and Transport			
Degree Program Degree Program in Environmental Technology			
Author Priscila Gandhi Estrada Reynoso			
Title of Thesis Further Development of a Centrifugal Solids Separator Prototype			
Date	9 May 2016	Pages/Appendices	78 / 2
Supervisors Mr. Pasi Pajula, Principal Lecturer and Mr. Teemu Räsänen, Lecturer			
Client Organization /Partners SansOx Ltd			

Abstract

This thesis was made for SansOx Ltd, part of the Finnish Cleantech cluster of companies, whose innovative ideas in the water treatment area have been awarded the WssTP Water Innovation SME Award for two consecutive years. The purpose of the thesis was to make a deeper theoretical research of the physical aspects related to solids separation in one of SansOx's innovations, a centrifugal solids separation device. Based on this research, it was aimed to make a review of the previous tests of the pilot-scale prototypes of the device as well as to develop a plan that would be the base for testing a prototype in a laboratory-scale.

The theory of solids separation in the device is strongly linked to hydraulics and particle settling, so the theoretical research was divided into three main subjects: physics and hydraulics, particle separation, and solid separation methods. Some basic principles of physics, such as vectors and forces, are the base for explaining the hydraulics related to fluid flow through pipes as well as for explaining the basic theory of particle settling. Solids separation methods were studied for a comparison between the commonly used methods in water treatment and SansOx's device. With the information of the theoretical research, a review of the conditions of the previous tests of the prototype could be made, as well as finding a cause for the results obtained in the tests. Lastly, the same calculations were used to develop the sizing and testing plan of a laboratory-scale prototype.

The results of the calculations showed that the main challenge in the previous testing of the prototypes was to achieve a discharge that would be high enough for separation. The parameters and calculations related to the solids separation were gathered into one single Excel workbook that would serve as a tool for designing a prototype depending on the characteristics of the solution to be treated. Finally, with this tool, a plan for the laboratory-scale prototype was developed.

Keywords
Water treatment, hydraulics, settling, solids removal, centrifugation

SAVONIA-AMMATTIKORKEAKOULU OPINNÄYTETYÖ
Tiivistelmä

Koulutusala Tekniikan ja liikenteen ala	
Koulutusohjelma Ympäristöteknologian koulutusohjelma	
Työn tekijä Priscila Gandhi Estrada Reynoso	
Työn nimi Keskipakovoimaan perustuvan kiintoaineenerotuslaitteen prototyypin jatkokehitys	
Päiväys 9.5.2016	Sivumäärä/Liitteet 78 / 2
Ohjaajat Yliopettaja Pasi Pajula ja lehtori Teemu Räsänen	
Toimeksiantaja/Yhteistyökumppani SansOx Oy	

Tiivistelmä

Opinnäytetyön tilaajana oli SansOx Oy, joka on yksi Suomen Cleantech -yrityksistä ja jonka innovatiiviset ideat on palkittu WssTP Water Innovation SME Award -palkinnolla kahtena peräkkäisenä vuonna. Opinnäytetyön tavoitteena oli tehdä teoriatarkastelu fysikaalisista ilmiöistä, jotka liittyvät SansOx:n kehittämään innovatiiviseen kiintoaineenerotusmenetelmään. Tarkasteltava menetelmä perustuu keskipakovoiman hyödyntämiseen, kun erotetaan kiintoainetta nestefaasista. Tehdyn teoriatarkastelun perusteella on mahdollista arvioida aikaisempien laitteistoprototyyppien toimintaa ja testauksen tuloksia. Teoriatarkastelu luo samalla perustan laitteiston laboratoriomittakaavaan kehitettävän version suunnittelutyöhön ja testaukseen.

Kiintoaineenerotuksen teoria liittyy vahvasti hydrauliikkaan ja partikkelin laskeutukseen, joten teoriatarkastelu oli jaettu kolmeen pääaiheeseen: fysiikka ja hydrauliikka, partikkelin erotus sekä kiintoaineenerotusmenetelmät. Fysiikan peruskäsitteet, kuten vektorit ja voimat, täydentävät putkessa virtaavan nesteiden hydrauliikan sekä partikkelin laskeutuksen teoriaa. Muita kiintoaineenerotusmenetelmiä tarkasteltiin, jotta kehitettyä laitteistoa voitiin verrata yleisesti vesien käsittelyssä käytettyihin menetelmiin. Teoriatarkastelun tietojen perusteella, voitiin arvioida aikaisempien prototyyppien toimintaedellytyksiä ja kyettiin löytämään selittäviä tekijöitä kenttäkokeissa saatuihin tuloksiin. Lopuksi, samoja laskelmia käyttäen pystyttiin kehittämään laitteiston seuraavan laboratoriomittakaavan prototyypin konstruktio ja testaussuunnitelma.

Laskelmien tulokset osoittivat, että laitteiston aikaisempien prototyyppien kenttäkokeiden keskeisenä haasteena oli riittävän suuren virtaaman aikaansaaminen laitteistoon. Kiintoaineenerotukseen liittyvät laskelmat ja niiden parametrit koottiin Excel-työkirjaan, joka voidaan hyödyntää jatkossa suunniteltaessa uusia laitteita erilaisiin kohteisiin. Lopuksi, saman Excel-työkirjan avulla laadittiin suunnitelma laitteiston laboratoriomittakaavan prototyypin konstruktioksi.

Avainsanat
Vedenkäsittely, hydrauliikka, laskeutus, kiintoaineenerotus, keskipakovoima

CONTENTS

1 INTRODUCTION

"Water is a limited natural resource and a public good fundamental for life and health. The human right to water is indispensable for leading a life in human dignity. It is a prerequisite for the realization of other human rights."

United Nations Committee on Economic, Social, and Cultural Rights (2002)

Water, as it is found in nature, rarely fulfills the quality requirements set for human use without previous treatment. Many human activities, from personal and domestic activities to industrial activities, can affect the quality and quantity of water. The purpose of water treatment is to provide safe water to human use, while taking into consideration aesthetical and technical issues. Aesthetical aspects include color, smell, and flavor, among others, while technical aspects are related to corrosion and damage of pipes and fittings. (RIL I 2003, 22, 41 - 43).

Global demographic and ecological challenges, like growing population, urbanization, and climate change, highlight the importance of wastewater treatment. People have a right to have access to safe water for personal and domestic use and, with limited water resources, the reuse of wastewater is a significant strategy. Wastewater treatment can also improve the quality of the raw water for water supply, so, with growing challenges, it is important to develop new and more effective technologies for water and wastewater treatment. (WHO 2015; RIL I 2003, 43 - 44).

SansOx Ltd., founded in 2012, is a company focused on developing innovative technologies in the water treatment area. It is part of the Finnish Cleantech cluster of companies and its innovations have been awarded for two consecutive years the WssTP Water Innovation SME Award in Brussels. SansOx's main product is an aeration device called OxTube, with which oxygenation can be achieved in less time and space compared to traditional aeration methods, requiring also less energy. (SansOx 2016).

Another of SansOx's innovations is a centrifugal solids separation device called SaoxFuge. The SaoxFuge is a spiral-shaped pipe in which solid particles are separated by the influence of the centrifugal force generated by high flow velocities. The first tests of a SaoxFuge pilot-sized prototype were carried out in the summer of 2014 with water and wastewater from different sources. These tests were followed by a second testing in the summer of 2015 with mine water from the apatite concentration plant in Yara Finland's Siilinjärvi site. Nevertheless, the results of the tests were inconclusive.

The purpose of this thesis is to perform a deeper theoretical research of the physical aspects related to solids separation in the SaoxFuge. This theoretical research will be the base for making a review of the 2015 tests of the SaoxFuge prototype in order to find out the possible causes of the inconclusive results of the tests. With the research and the conclusions of the review of the past tests it is aimed to develop a plan for designing and testing a SaoxFuge laboratory-sized prototype for having more control over the conditions of the tests.

The theoretical research in this thesis is divided into three main subjects: physics and hydraulics, particle separation, and solids separation methods, which are the subjects that are strongly linked to the theory of solids separation in the SaoxFuge. The hydraulics theory is focused on flow through pipes, while the particle separation theory focuses on particle settling. Both are complemented by the theory of basic physical concepts, like vectors and forces. The solids separation methods are studied for a better understanding of the commonly used methods in water treatment as well as for a comparison between some of them and the SaoxFuge.

The review and analysis of the previous tests of the prototypes takes the basic and general principles of the subjects dealt with in the theoretical part of the thesis while also making some assumptions for different calculations. The results of the calculations are used to consider possible reasons for the inconclusive results of the tests.

With the same calculations, a plan is developed for the laboratory-scale prototype dimensions and optimal testing conditions. The plan takes into consideration the particle sizes and densities most commonly found in water and wastewater treatment facilities and its purpose is to pay attention to the main parameters affecting the solids separation. As an aid for this, the calculations are gathered into a single Excel workbook containing the parameters and formulas used in the development of this plan.

Finally, it is important to clarify that the theories and calculations in this thesis serve as a general guide for the design and testing of the prototype. More accurate and deeper investigation of the phenomena occurring in the SaoxFuge can be done with the study of further literature and the use of more advanced tools, like numerical analysis or tomography.

2 PHYSICS AND HYDRAULICS

2.1 Vectors

A vector is a physical quantity that requires not only a magnitude and a unit but also a direction to be described, unlike scalar quantities, which are described only by their magnitude and unit. Such physical vector quantities are for example velocity, acceleration, and force, among others. (Benson 1995, 16).

The graphical representation of vectors is made either with bold letters or using an arrow on top of the letters. For example, the acceleration vector can be represented as $\boldsymbol{a}$ or as $\vec{a}$. If it is only referred to the magnitude of a vector, it can be represented by using its letter without the arrow or with absolute value signs. For example a or $|\vec{a}|$. The geometric representation of a vector is an arrow whose size is proportional to the magnitude of the vector and its angle and arrow tip show its direction (Figure 1). A vector can be moved to any point in space without changing as long as its magnitude and direction remain the same. (Benson 1995, 17; Croft, Davison & Hargreaves 2001, 203).

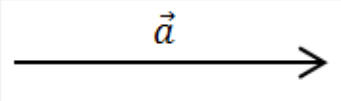

FIGURE 1. Vector $\vec{a}$

For making calculations with vectors, vector algebra is used. Some of the basic vector calculations used in this thesis will be described next.

2.1.1 Vector addition, subtraction and multiplication by a scalar

The sum of two or more vectors is called a resultant and these vectors become the resultant components. The graphical sum of a vector is made by moving the vectors so that the end of one of the vectors is the starting point of the next one. The resultant will be the vector that joins the starting point of the first vector with the ending point of the last vector (Figure 2). Figure 2 also shows that vector addition is commutative. (Benson 1995, 19; Tuomenlehto, Holmlund, Huuskonen, Makkonen Surakka 2014, 169).

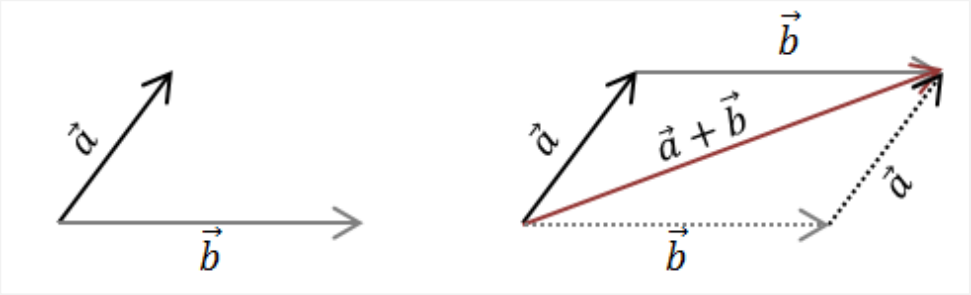

FIGURE 2. Graphical addition of two vectors

When adding two vectors, a triangle is formed and thus the resultant magnitude can be calculated using trigonometrical calculations. When more than two vectors are added, the calculation can be broken into smaller triangles by adding two vectors and then adding one vector at a time to the previous resultant (Figure 3). (Knight 2014, 83 - 84).

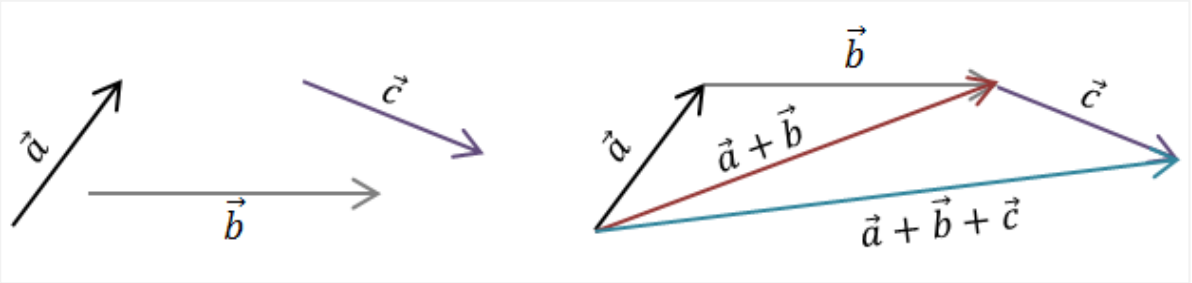

FIGURE 3. Addition of three vectors

The subtraction of a vector is made by adding an opposite vector (Figure 4). Two vectors are opposite when they have the same magnitude but opposite direction. The opposite vector of a vector is represented with a minus sign before it (-). (Benson 1995, 17, 19).

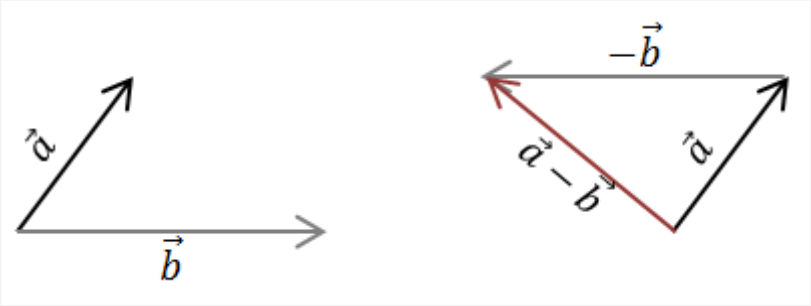

FIGURE 4. Vector subtraction

When a vector is multiplied by a scalar, the scalar magnitude affects the vector magnitude and the scalar sign affects the vector direction. In other words, a positive scalar will change only the vector magnitude while a negative scalar will change not only the vector magnitude but also its direction to an opposite direction (Figure 5). The vector multiplication by a scalar is commutative, distributive, and associative. (Croft et al. 2001, 208).

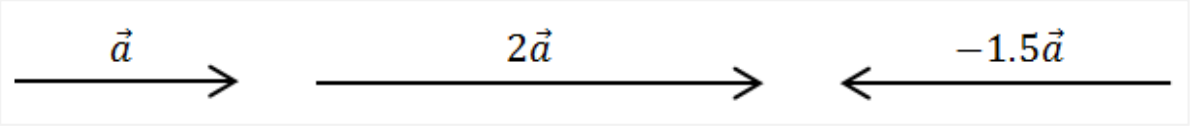

FIGURE 5. Multiplication of a vector by a scalar

2.1.2 Coordinate representation

A unit vector is a vector whose magnitude is one and provides a direction in space. In a Cartesian coordinate system, the unit vectors $\vec{\imath}$, $\vec{\jmath}$ and $\vec{k}$ represent the direction in the *x*, *y*, and *z* axes respectively (Figure 6). A vector can be represented in a coordinate system using its components in the $\vec{\imath}$, $\vec{\jmath}$, and $\vec{k}$ directions and thus the vector can be defined as the sum of these vectors. In Figure 7, the components $\vec{\imath}$ and $\vec{\jmath}$ of vector $\vec{a}$ are shown. (Benson 1995, 21).

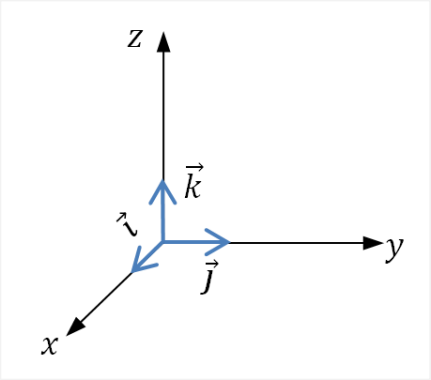

FIGURE 6. Unit vectors in a Cartesian coordinate system

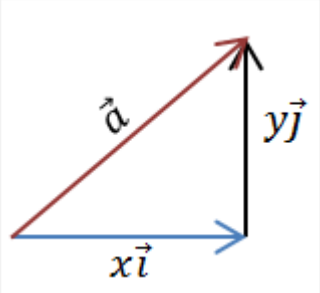

FIGURE 7. $\vec{\imath}$ and $\vec{\jmath}$ and components of vector $\vec{a}$

2.2 Force

Newton's second law states that an object of mass *m* that is subject to a net or total force $\vec{F}$ will have an acceleration $\vec{a}$. In other words, the total force acting on an object is the product of the acceleration of the object times its mass (Eq. 1). Also, as Newton's first law states, if the net force is equal to zero, then the object will remain at rest or will continue to move at a constant velocity. (Knight 2014, 144 - 146).

$$\sum \vec{F} = m\vec{a} \qquad \text{(Eq. 1)}$$

In the next three chapters, some of the main forces acting in the separation processes reviewed in this work are described.

2.2.1 Gravitational force

In his law of gravity, Newton recognized that two objects of mass m_1 and m_2 respectively exert on each other an attractive force that is inversely proportional to the square of the distance r between them. This attraction force can be determined by:

$$F_{12} = F_{21} = \frac{G\, m_1 m_2}{r^2} \qquad \text{(Eq. 2)}$$

where G is the gravitational constant of magnitude 6.67 x 10^{-11} Nm^2/kg^2. This value is so small that attraction forces between common objects are negligible. On the other hand, this attraction force becomes significant when considering an object of large mass, like a planet or other celestial objects. (Knight 2014, 167).

The attraction force or gravitational force $\vec{F}_G$ that a planet has on an object near it can be calculated with Equation 2 using the average mass and radius of the planet and the mass of the object. The result of this is known as the object's weight W. However, considering Newton's second law (Eq. 1), the following can be deduced (Eq. 3): (Knight 2014, 167).

$$\vec{F}_G = \frac{G\, M_{planet}\, m}{R^2} = m\vec{a} \qquad \text{(Eq. 3)}$$

$$\vec{a} = \frac{G\, M_{planet}}{R^2} = g \qquad \text{(Eq. 4)}$$

Equation 4 shows that the gravitational force of a planet causes an acceleration g (the so-called free-fall acceleration) of the object. This acceleration is a property related to the planet and is the same for any object on the planet. For planet Earth, g can be calculated like this: (Knight 2014, 167).

$$g = \frac{\left(6.67 * 10^{-11}\, \frac{N\, m^2}{kg^2}\right)(5.98 * 10^{24}\, kg)}{(6.37 * 10^{6}\, m)^2} \approx 9.83\, \frac{m}{s^2}$$

For future use, the value of g will be 9.81 m/s^2, considering a slight loss due to the rotation of the planet. The direction of this acceleration, and consequently of the gravitational force, is always towards the center of the planet, downwards. Also, for analyzing objects that are very close to the planet's surface, the curvature of the planet is not relevant and in most cases its surface can be considered flat. (Knight 2014, 167 - 168).

2.2.2 Centrifugal force

The centrifugal force is a so-called fictitious or apparent force, that is, a force that cannot be described within an inertial reference frame. Inertial reference frames are those in which Newton's laws are valid, for example, a frame that is at rest or at constant velocity, but not an accelerating reference frame. Centrifugal force, thus, describes from a non-inertial reference frame the outward throw a body is subject to when moving in a circular pattern (accelerating reference frame) (Figure 8). (Knight 2014, 147, 229 – 230)

The centrifugal force can be calculated with Equation 5, where v is the tangential velocity of the body, and r is the radius of the circular pattern. ω is the angular velocity of the body in rad/s (Knight 2014, 116, 231). The centrifugal acceleration that the body is subject to relative to the gravitational acceleration of the Earth is called G (RIL II 2003, 103).

$$\vec{F}_C = \frac{m\,v^2}{r} = m\omega^2 r \qquad \text{(Eq. 5)}$$

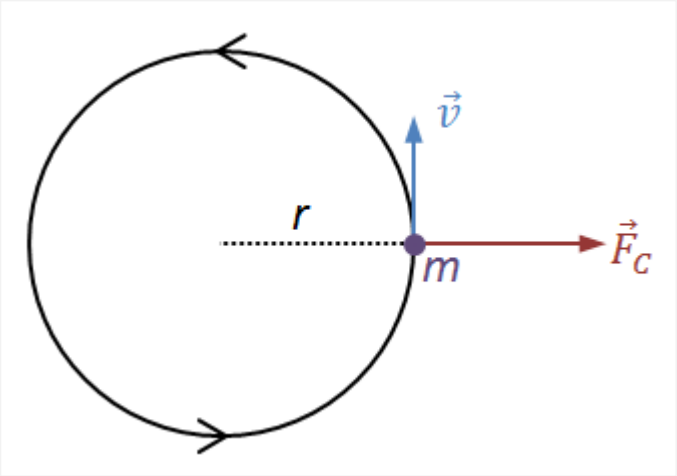

FIGURE 8. Centrifugal force in a circular pattern

2.2.3 Drag force

Drag force is a resistive force that is opposite to the direction of motion of a body in a fluid and is related to the speed of the body. This resistive force depends also on the shape of the body and the density of the fluid as well as the type of flow around the body (Chapter 2.4). (Benson 1995, 110).

For a laminar, steady flow around a slow body, the resistance to motion is closely related to the friction between the fluid and the body and so, the drag force is directly proportional to the speed of flow as seen in Equation 6, where γ is a constant dependent of the dimension of the body and the viscosity of the fluid. (Benson 1995, 110).

$$\vec{F}_D = \gamma v \qquad \text{(Eq. 6)}$$

On the other hand, for turbulent flows around a large or fast body, there is difference in pressure in front and behind the moving object and so other factors affect the magnitude of the drag force. In this case, the drag force is directly proportional to the square of the velocity of the object and can be expressed as in Equation 7:

$$\vec{F}_D = \frac{1}{2} C_D \rho A v^2 \qquad \text{(Eq. 7)}$$

where C_D is the drag coefficient that depends on the shape of the object and its orientation, ρ is the density of the fluid and A is the cross-section area (a two-dimensional projection) of the object (Figure 9). (Benson 1995, 111).

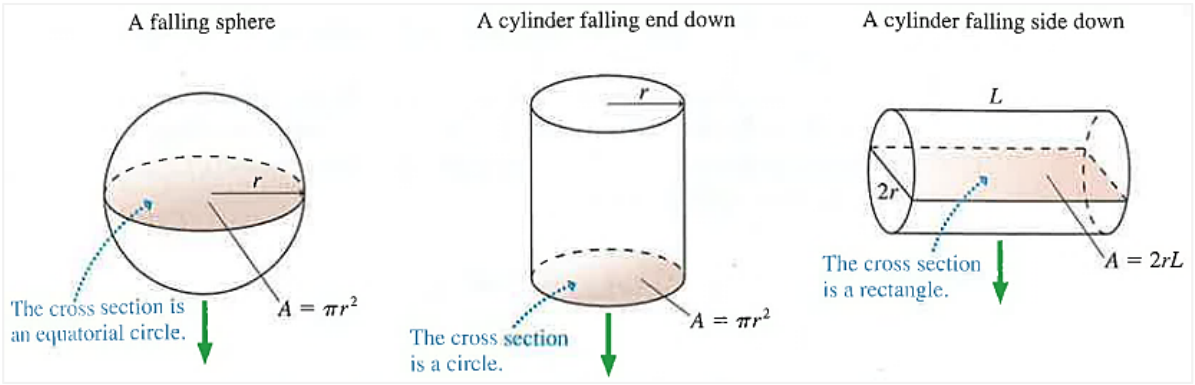

FIGURE 9. Cross-section areas for objects of different shape (modified from Knight 2014, 175)

2.3 Properties of fluids

2.3.1 Density

Mass density ρ is defined as the mass and volume ratio of a substance (Eq. 8). The density of fluids can vary with temperature and pressure, although the latest is more significant to gases than to liquids. For water, a maximum density of 1000 kg/m^3 is reached at 4 °C. The relative density of a substance is the relation of its density and the density of water at 4 °C. (Benson 1995, 285). Table 1 shows the water density value at different temperatures at atmospheric pressure.

$$\rho = \frac{m}{V} \qquad \text{(Eq. 8)}$$

TABLE 1. Density of water at different temperatures and atmospheric pressure (Tchobanoglous, Stensel, Tsuchihashi, Burton, Abu-Orf, Bowden & Pfrang 2014, 1915)

Temperature (°C)	Density (kg/m³)
0	999.8
5	1000.0
10	999.7
15	999.1
20	998.2
25	997.0
30	995.7
40	992.2
50	988.0
60	983.2
70	977.8
80	971.8
90	965.3
100	958.4

2.3.2 Pressure

In fluids, molecular movement causes molecules to collide with their surroundings, which exerts a normal force on the impacted objects. The average force of all the collisions per unit area is defined as pressure (Eq. 9). This force can be also caused by gravity and thus the weight of the fluid causes pressure. Considering the weight of a column of fluid of height *h*, pressure can be expressed as in Equation 10. (Knight 2014, 462; Hamill 2011, 6).

$$P = \frac{F}{A} \qquad \text{(Eq. 9)}$$

$$P = \rho g h \qquad \text{(Eq. 10)}$$

The pressure caused by the weight of the air in the atmosphere is known as atmospheric pressure and its maximum value is reached at sea level. The average value taken for the atmospheric pressure is 1.013 MPa. Usually, when measuring the pressure of a fluid, atmospheric pressure is not considered and therefore the measured pressure is called gauge pressure. The sum of the atmospheric pressure and the gauge pressure is defined as absolute pressure. (Hamill 2011, 7 - 8).

2.3.3 Viscosity

Viscosity is one of the most relevant properties of a fluid when it comes to flow. The viscosity of a fluid is its resistance to shear stress, in other words, its resistance to flow due to internal friction (Hamill 2011, 75).

Newton studied viscosity by placing a liquid between two horizontal plates and moving the upper plate by pulling it horizontally. This causes a deformation of the liquid because the liquid sticks to both the moving and the stationary plate (Figure 10). (Hamill 2011, 76 - 77).

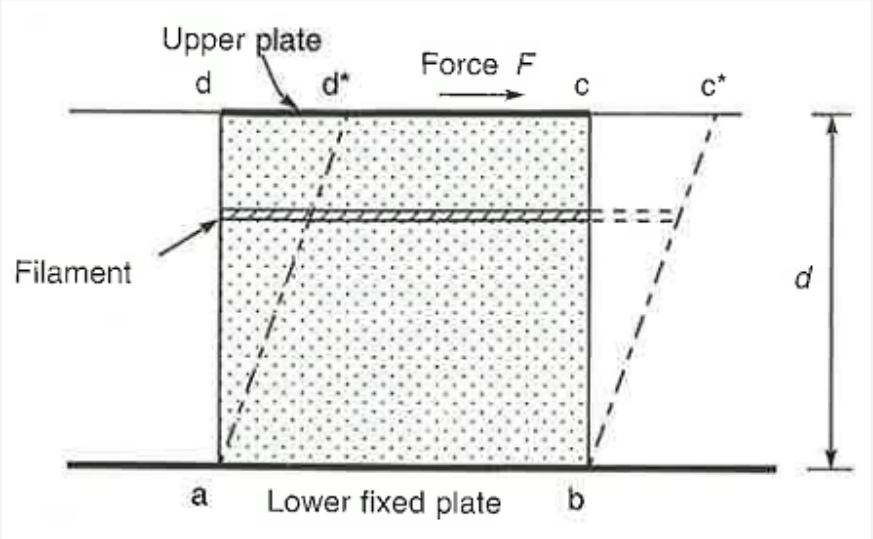

FIGURE 10. Liquid between two plates (modified from Hamill 2011, 76)

The force needed to move the plate divided by the area of the plate is the shear stress τ on the liquid. In Chapter 2.3.2 pressure was also defined as the relation between force and area. The difference between pressure and shear stress lies in the fact that the force in pressure is a normal force (perpendicular to the surface) while shearing force is tangential (parallel to the surface). (Hamill 2011, 76)

Newton realized that the force needed to move the plate is proportional to the area *A* of the plate, the velocity *v* of the plate, and the distance *d* between both plates according to Equation 11:

$$F = \mu \frac{A\,v}{d} \qquad \text{(Eq. 11)}$$

where the constant μ is the dynamic viscosity of the fluid. Based on equation 8, shear stress can also be expressed as Equation 12. (Hamill 2011, 77).

$$\tau = \mu \frac{v}{d} \qquad \text{(Eq. 12)}$$

Dynamic viscosity is constant at a certain temperature and it varies with temperature, like density. For most of the liquids, the effect of pressure in viscosity is negligible compared to the effect of temperature. Only for some mineral and synthetic oils an increment in pressure causes a considerable increment of viscosity. Water under 32 °C, unlike other liquids, has a decrease in viscosity with an increase of pressure. Above 32 °C its viscosity increases with increasing pressure. (Mezger 2006, 72). In Table 2 and 3 is presented the viscosity of water at different temperatures and pressures.

Viscosity can be also expressed as kinematic viscosity *v*, which refers to the ratio of dynamic viscosity and density and, therefore, whose units are expressed as m^2/s (Hamill 2011, 77).

TABLE 2. Viscosity of water at different temperatures and atmospheric pressure. (Tchobanoglous et al. 2014, 1915)

Temperature (°C)	Dynamic viscosity $*10^3$ (Ns/m^2)
0	1.781
5	1.518
10	1.307
15	1.139
20	1.002
25	0.890
30	0.798
40	0.653
50	0.547
60	0.466
70	0.404
80	0.354
90	0.315
100	0.282

TABLE 3. Effect of pressure upon viscosity (modified from Forsythe 1954; 2003, 334)

Temperature (°C)	Absolute viscosity at 1 atm (cP)	Relative viscosity				
		Pressure in kg/cm^2				
		1	1000	4000	8000	12000
0	1.792	1.0	0.921	1.111	freezes	-
10.3	1.297	0.779	0.743	0.842	1.152	-
30	0.801	0.488	0.514	0.658	0.923	1.206
75	0.380	0.222	0.239	0.302	0.445	-
100	0.284	-	-	-	-	-

2.4 Pipe flow

Fluid flow through pipes has a great significance not only to the industry but also to the community. According to the World Health Organization (WHO 2015), the water supply of 4.2 billion people around the world is done through pipelines.

Fluid flow can be laminar or turbulent. In laminar flow, viscosity dominates the flow making the fluid particles move one after another slowly and uniformly. Because of friction, at the pipe walls the flow velocity is zero but increases as the distance from the pipe walls increases, reaching a maximum velocity in the middle of the pipe and remaining somewhat constant in a particular point in the pipe as time goes by. The maximum velocity in laminar flow is about two times greater than the mean

velocity of the flow (Figure 11). Nevertheless, this type of flow is rather unusual. (Hamill 2011, 80 - 81).

On the other hand, turbulent flow is the most common type of flow, especially in the means of water supply. In this kind of flow, particles move fast and randomly, each in its own path. Here, flow velocity at the walls of the pipe is also zero and increases to the center of the pipe, with the difference that the change is not uniform and velocity in a certain point of the pipe varies from time to another (Figure 11). In addition, the maximum velocity is only about 1.7 times the average velocity, due to the velocity of the particles in directions that vary from the direction of the flow. These transverse velocities have a mixing effect in the flow. (Hamill 2011, 80 - 81).

Between these two kinds of flow there is a middle stage called transitional flow, where the smooth paths of particles of the laminar flow start to break up into a more chaotic flow (Hamill 2011, 183).

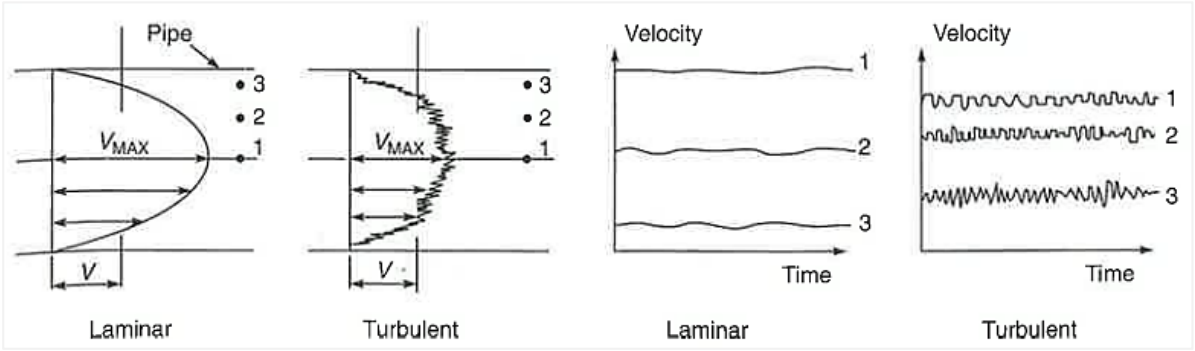

FIGURE 11. The difference between laminar and turbulent flow illustrated diagrammatically (modified from Hamill 2011, 81)

In addition to this, when the channel of flow is curved and the velocity of flow is large enough, the flow is stabilized by secondary motions that are generated due to the influence of centrifugal force. The maximum velocity of the flow is at the center of the pipe and, thus, when starting to flow in a curved path, the centrifugal force is greater at this point. Then again, the centrifugal force is lowest in the outer wall of the curvature, where the flow velocity is smaller and the radius of curvature larger. Due to the centrifugal force, the fluid at the center of the pipe moves towards the outer side of the curvature and is replaced by fluid coming from the inner side of the curvature. (Kundu, Cohen & Dowling 2012, 825 - 826).

The secondary motions create two vortices known as the Dean vortices (Figure 12), which influence the axial flow inside the pipe. William Reginald Dean (1928) developed a series of equations for studying these secondary motions (hence the name of Dean vortices). In these equations, a parameter known as the Dean number (De) is used for modifying the Reynolds number (Chapter 2.4.1) by the curved pipe. De depends on the Reynolds number, the diameter of the pipe, and the radius of curvature. Usually numerical analysis and computational fluid dynamics (CFD) are required for detailed studies of the structure of this type of flow. (Kundu et al. 2012, 825 - 831).

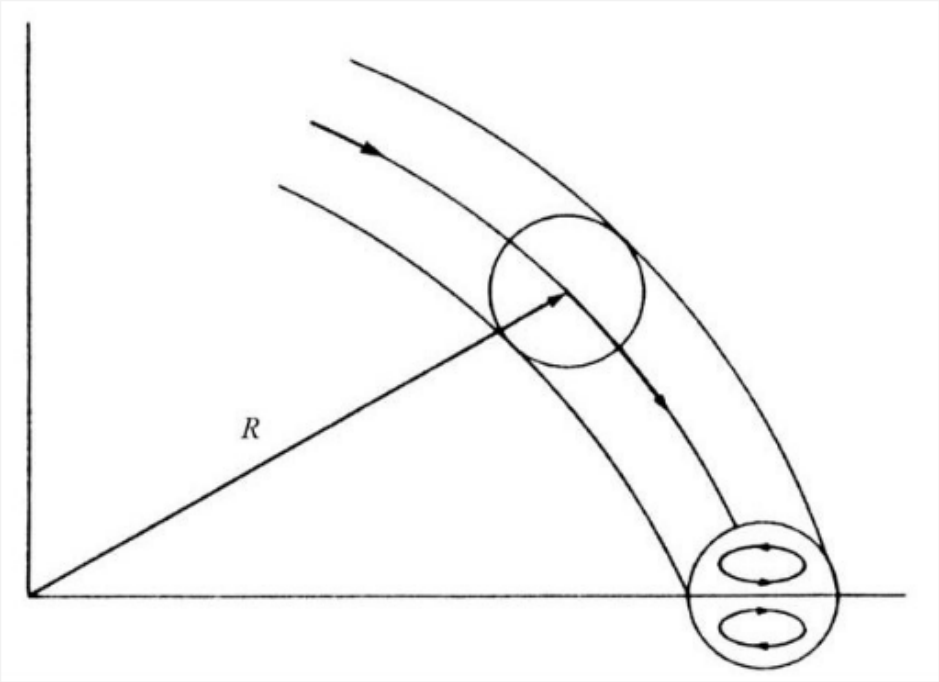

FIGURE 12. Schematic of flow in a curved tube (Kundu et al. 2012, 826)

2.4.1 Reynold's number

In the 1880s, Osborne Reynolds made a series of experiments to determine the factors that influence the type of flow. The experiment consisted of injecting a thin stream of dye into liquid flowing through a pipe. By varying flow velocity with the help of a valve at the downstream end as well as using different pipe diameters and liquids, he observed the point at which the stream of dye started to break up and mix with the liquid. With his experiments, Reynolds found out that the type of flow is determined by the velocity V of the flow, the dynamic viscosity μ and density ρ (or kinematic viscosity ν) of the liquid and also the diameter d of the pipe according to Equation 13: (Hamill 2011, 184)

$$Re = \frac{\rho V d}{\mu} \qquad \text{(Eq. 13)}$$

Re is a dimensionless number that serves as a general guide to know the type of flow in certain conditions. It shows the relation between inertial and viscous forces. For water, the rough values of Re for laminar, transitional, and turbulent flow in pipes are given in Table 4. (Hamill 2011, 80 - 81; Graebel 2001, 276).

TABLE 4. General values of Re for water pipe flows (Hamill 2011, 183)

Type of flow	Re
Laminar	< 2000
Transitional	2000 < Re < 4000
Turbulent	> 4000

2.4.2 Continuity equation

The law of conservation of mass states that, since matter cannot be created nor destroyed, the total mass in a closed system is constant. In other words, within an analyzed system, the amount of mass entering the system is equal to the sum of the amount of mass that exits the system and the amount of mass that remains in the system. (Graebel 2001, 126).

Considering a pipe as a closed system and supposing the pipe is completely full of water, so the amount of mass accumulated in the system remains constant, the amount of water entering the pipe equals the amount of water exiting the pipe. The mass flow rate entering or exiting the pipe can be calculated by multiplying the volumetric discharge Q by the density ρ of the water. The volumetric discharge can also be expressed in terms of velocity and area (Eq. 14). Assuming the density of the water remains fairly constant within the pipe, the conservation of mass can be expressed as in Equation 14, also known as the continuity equation.

$$Q_1 = A_1 v_1 = A_2 v_2 = Q_2 \qquad \text{(Eq. 14)}$$

where Q_1 and Q_2 are the entering and exiting volumetric discharges, A is the cross-sectional area of the pipe and v the mean velocity of the fluid. Since volumetric discharge is the same at the entrance and exit of the pipe, a change in the cross-sectional area of the pipe will affect the velocity of the fluid. (Hamill 2011, 86).

2.4.3 Bernoulli equation

The law of conservation of energy, just as the law of conservation of mass, states that energy cannot be created nor destroyed, only transformed. Thus, the amount of energy entering a system equals the energy accumulated in the system plus the energy exiting the system. (Graebel 2001, 133).

In hydraulics, there are three main types of energy to be considered: the potential energy, the kinetic energy, and the pressure energy. The potential energy of a fluid is the result of a change in height from a reference point. The higher the fluid is raised, the greater its potential energy. Potential energy can be calculated with Equation 15, where h is the height between the fluid and the reference point. (Hamill 2011, 103; RIL I 2003, 137).

$$E_P = mgh \qquad \text{(Eq. 15)}$$

The kinetic energy of a fluid is due to the motion of the fluid and thus can be calculated using the velocity of the fluid (Eq. 16). Finally, a fluid under pressure has pressure energy, which origins from the fact that if a fluid in a full pipe with constant diameter has a decrease in potential energy, it cannot increase its kinetic energy (because of the conservation of mass) and, thus, the potential energy transforms into pressure energy. The pressure energy of a fluid can be calculated with Equation 17,

where *p* is the pressure of the fluid, *A* is the cross-sectional area of the pipe and *L* is the distance that the fluid has travelled. (Hamill 2011, 103).

$$E_K = \frac{1}{2} mv^2 \qquad \text{(Eq. 16)}$$

$$E_p = pAL = pV = \frac{p\,m}{\rho} \qquad \text{(Eq. 17)}$$

The total energy in the pipe is the sum of the three types of energy and it has to remain constant in both ends of the pipe analyzed. Also, the amount of energy is usually expressed per unit weight of fluid ($W = mg$), and therefore its unit is expressed in meters. The energy terms given in meters are called heads: the elevation, velocity, and pressure heads. The amount of energy between two points in a pipe can be expressed as in Equation 18, the so-called energy equation or Bernoulli equation: (Hamill 2011, 103 - 105, 164; RIL I 2003, 137)

$$h_1 + \frac{v_1^2}{2\,g} + \frac{p_1}{\rho\,g} = h_2 + \frac{v_2^2}{2\,g} + \frac{p_2}{\rho\,g} \qquad \text{(Eq. 18)}$$

The last equation is valid assuming there are no energy losses due to factors like friction or bends, among others. Hence, for a real fluid and flow, the energy head losses term (h_f) can be added to the Bernoulli equation and be expressed as in Equation 19. In Chapter 2.4.4 head losses calculation is described. (Hamill 2011, 105).

$$h_1 + \frac{v_1^2}{2\,g} + \frac{p_1}{\rho\,g} = h_2 + \frac{v_2^2}{2\,g} + \frac{p_2}{\rho\,g} + h_f \qquad \text{(Eq. 19)}$$

Figure 13 shows the relationship between these terms and the total energy. In a stand-pipe (or piezometer), water rises due to the elevation and the pressure heads. The level of this piezometric head is known as the hydraulic grade line and is lower than the total head line. The difference between the two is given by the velocity head. One main difference between the hydraulic grade line and the total head line is that the latter always decreases towards the direction of flow because of head losses, whereas the hydraulic grade line can decrease or increase depending on the changes in pipe diameter (changes in velocity of flow). (Hamill 2011, 164 - 165).

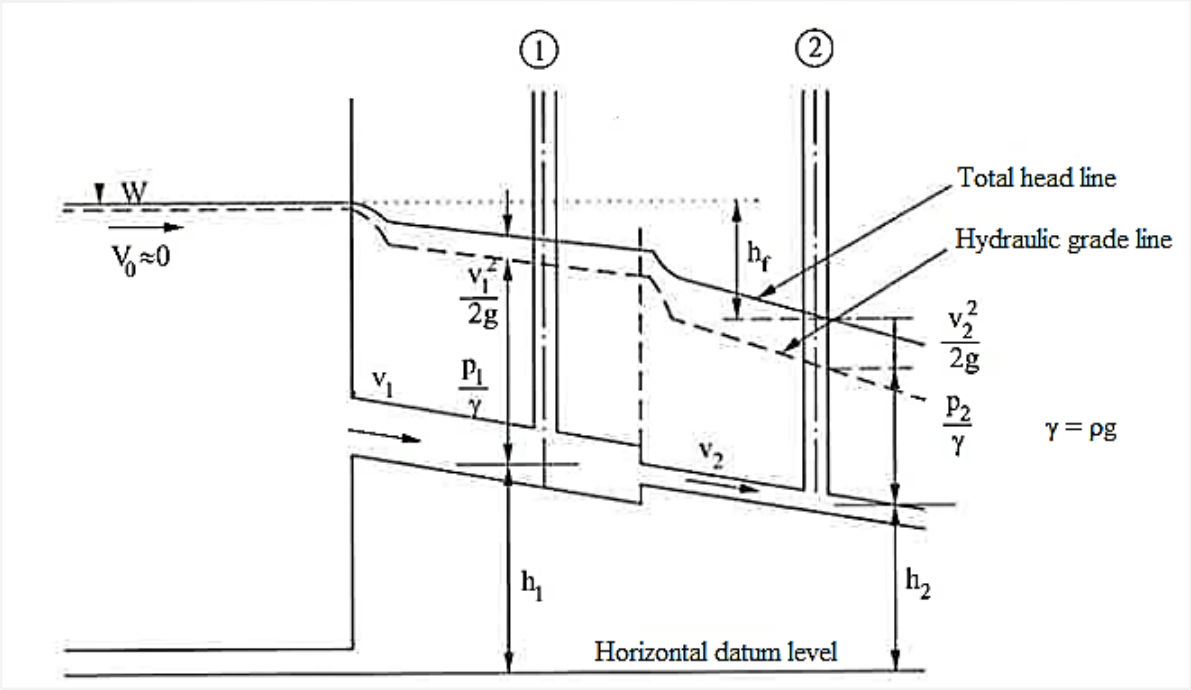

FIGURE 13. Water pipe flow and its energy types (modified from RIL I 2003, 137)

2.4.4 Head loss

The head losses (h_f) mentioned in the previous chapter can be caused by friction between the water and the pipe (friction losses), or minor losses caused by changes in the cross-sectional area of flow, pipe diameter, bends, and fittings. Usually, friction losses would be more significant in long pipes, while minor losses would be more significant in short pipes. (Hamill 2011, 169).

Some of the methods and equations for calculation of the head losses will be described next.

Poiseuille equation

In the 1840's, Jean Louis Poiseuille developed an equation for the calculation of friction loss in laminar flow (Eq. 20). In this type of flow, head losses due to friction are proportional to the velocity of the flow and pipe roughness does not affect the flow, so in Poiseuille's equation is expressed that head losses h_F in laminar flow depend on the kinematic viscosity v of the fluid, the length L and diameter D of the pipe, and the mean velocity V of the flow. (Hamill 2011, 185).

$$h_F = \frac{32\, v\, L\, V}{g\, D^2} \qquad \text{(Eq. 20)}$$

Darcy-Weisbach equation

Around 1850, Henry Darcy and Julius Weisbach developed an equation for determining head losses in full pipes. Unlike in laminar flow, the head loss in turbulent flow is directly proportional to the square of the velocity. The Darcy-Weisbach equation considers this and also the effect of pipe roughness on the flow (Equation 21).

$$h_F = \frac{f\,L\,V^2}{2\,g\,D} \qquad \text{(Eq. 21)}$$

where *f* is the pipe friction factor, *L* is the length of the pipe, *V* is the mean velocity of the flow, and *D* is the inner diameter of the pipe. (Hamill 2011, 185; RIL I 2003, 140).

The friction factor value depends mainly on the Reynolds number and the relative pipe roughness. For laminar flow, the viscosity of the fluid is the main factor affecting the friction factor, so equating the Poiseuille equation with the Darcy-Weisbach equation, the friction factor can be calculated with Equation 22: (Hamill 2001, 186)

$$f = \frac{64\,v}{D\,V} = \frac{64}{Re} \qquad \text{(Eq. 22)}$$

Johann Nikuradse experimented in 1933 the effect of pipe roughness on head loss by gluing grains of sand of known size (*k*) to the walls of a pipe and measuring the discharge. The relation between the size of the grains of sand and the diameter of the pipe is known as the relative roughness of the pipe. The results of these experiments were later compared to the results of tests with commercial pipes. In 1938-1939, Frank Colebrook realized that Nikuradse's experiment results could be expressed with the formula in Equation 23. Lewis Moody graphed in 1944 the results of this formula, resulting in what is called the Moody diagram (Figure 14), which can be used to determine the friction factor *f*. (Graebel 2001, 354; Hamill 2011, 186 - 187).

$$\frac{1}{\sqrt{f}} = -2\log\left(\frac{k}{3.7\,D} + \frac{2.51}{Re\,\sqrt{f}}\right) \qquad \text{(Eq. 23)}$$

The Moody diagram shows the friction factor values for the laminar flow (Eq. 22), as well as a critical zone, and three different zones of turbulent flow: the smooth turbulent flow, the transitional turbulent flow, and the rough turbulent flow (Graebel 2001, 354).

The critical zone corresponds to Reynolds number values of 2300 to about 4000, where the type of flow is transitional, and thus it is difficult to determine accurately the friction factor in this area. The smooth turbulent flow zone is at the bottom of the diagram. In this, the pipe roughness does not have yet significance and the curve depends on the Reynolds number. In the transitional turbulent flow, the curves of different relative roughness values start to separate from the smooth turbulent flow curve, so both the Reynolds number and the relative roughness of the pipe affect the friction factor

value. Finally, in the rough turbulent flow zone, the curves are practically horizontal and thus, the friction factor depends only on the relative pipe roughness. (Graebel 2001, 354; Hamill 2011, 187 - 188).

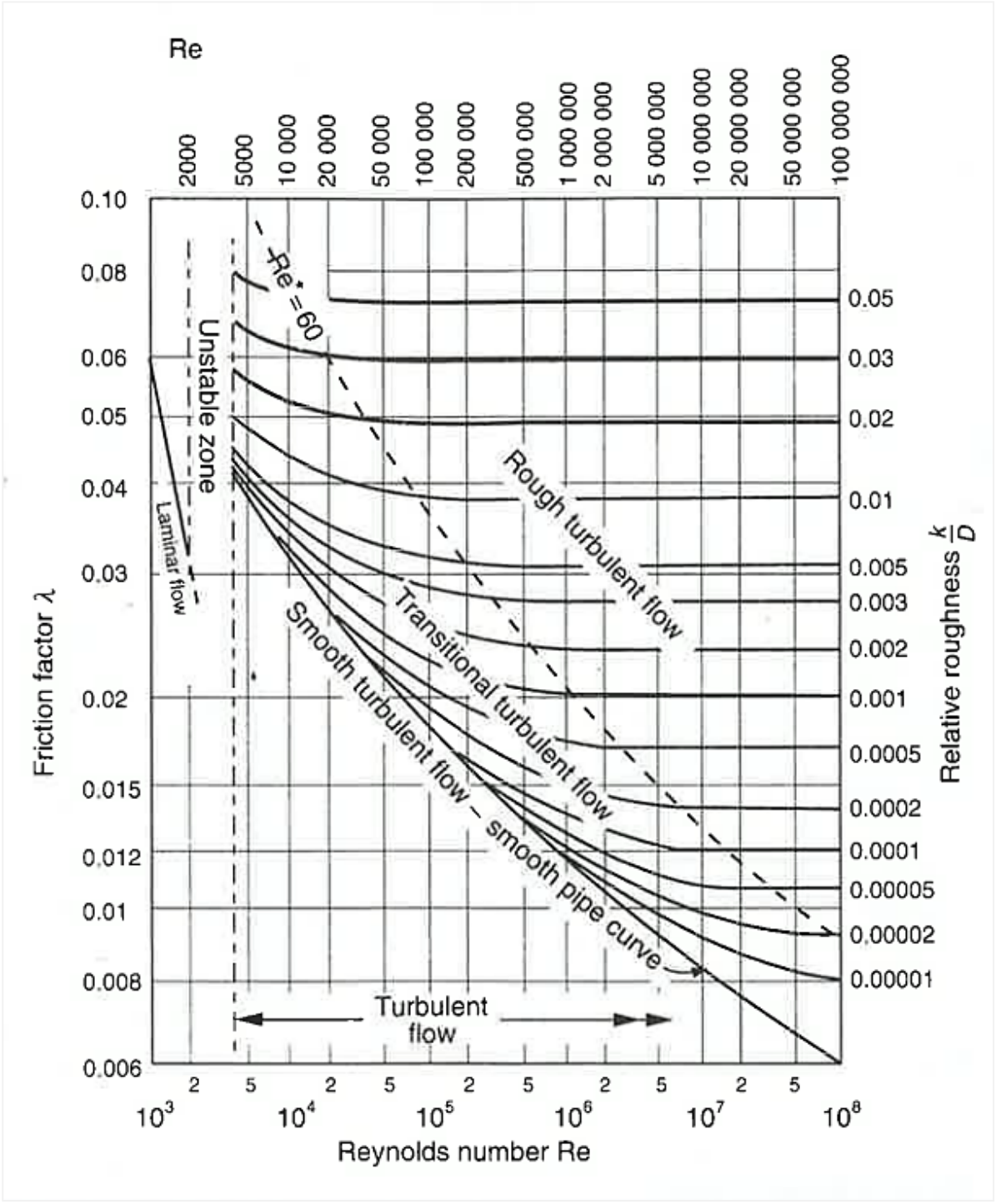

FIGURE 14. Moody diagram (Hamill 2011, 187)

Hazen-Williams equation

Because of its simplicity, the Hazen-Williams equation (Eq. 24) is widely used, especially in the water supply area. This empirical formula is fairly accurate with pipe diameters greater than 50 mm, flow velocities below 3 m/s, and a Hazen-Williams coefficient (C_{HW}) above 100. This coefficient depends

on velocity and on the diameter, material, and age of the pipe. Table 5 shows some of the values of C_{HW} for different pipes. (RIL I 2003, 142; Hamill 2011, 199).

$$Q = 0.278\, C_{HW}\, D^{2.63} \left(\frac{h_F}{L}\right)^{0.54} \qquad \text{(Eq. 24)}$$

TABLE 5. Hazen-Williams C_{HW} coefficient values (RIL I 2003, 145)

Pipe material	C_{HW}
Asbestos-cement	140
Concrete	120-140
Galvanized pipe	120
Copper	130-140
Brass	130-140
Plastic	140-150
Steel	110-120
Cast iron (new)	130
Cast iron (5 years old)	120
Cast iron (10 years old)	107-113
Cast iron (20 years old)	89-100
Cast iron (30 years old)	75-90
Cast iron (40 years old)	64-83

Manning equation

Another way of determining the head losses is with the Manning formula (Eq. 25) which is usually used for calculations in open flow channels, like sewers, but that can be also applied to flow in full pipes. For this full pipe flow, the hydraulic radius *R*, that is, the cross-sectional area and wetted perimeter ratio, equals to D/4. (Hamill 2011, 199).

$$V = \frac{1}{n}\, R^{\frac{2}{3}} \left(\frac{h_F}{L}\right)^{\frac{1}{2}} \qquad \text{(Eq. 25)}$$

The coefficient *n* is known as the Manning or roughness coefficient and its value, depending on the material of the surface, is between 0.009 and 0.040 $s/m^{1/3}$, although for some open channel flow cases it can be of about 0.200 $s/m^{1/3}$ (RIL I 2003, 145; Hamill 2011, 233). Some of the values of *n* of different pipe materials are presented in Table 6.

TABLE 6. Common values for the Manning roughness coefficient *n* (modified from RIL I 2003, 147)

Surface material	n ($s/m^{1/3}$)
Brass pipe	0.009 – 0.013
Cast iron pipe	0.010 – 0.014
Plastic pipe	0.008 – 0.010
Concrete pipe	0.011 – 0.014

Minor losses

Minor head losses are caused by changes in pipe diameter and cross-sectional area, as well as fittings like valves and bends. Although called minor losses, these head losses can be of great significance, especially in short pipes. (Hamill 2011, 169).

Minor losses h_L are usually calculated with Equation 26, where K is the resistance coefficient, and V is the velocity of the flow. The value of K depends on the type of change and fitting and it is given in tables and also by manufacturers. Some of the values of K for different fittings are given in Table 7. Sometimes these losses are also expressed as l/D or added length of straight pipe, that is, the head loss given by a certain length l of straight pipe of diameter D that equals the head loss given by the fitting. (Hamill 2011, 204 - 205; RIL I 2003, 151).

$$h_L = K \frac{V^2}{2g} \qquad \text{(Eq. 26)}$$

TABLE 7. Head losses caused by changes in geometry and fittings to pipelines (modified from Hamill 2011, 205)

Loss	K	l/D (approx.)
Sharp edged entrance	0.50	22
Slightly rounded entrance	0.25	11
Bend – with r/D = ½		
22.5° bend	0.20	9
45° bend	0.40	18
90° bend	1.00	45
Bend with r/D = 1		
22.5° bend	0.10	5
45° bend	0.20	9
90° bend	0.40	18
Bend with r/D = 8 to 50		
22.5° bend	0.05	2
45° bend	0.10	5
90° bend	0.20	9
Gate valve		
fully opened	0.12	6
quarter closed	1.00	45
half closed	6.00	270
three-quarters closed	24.00	1080
Sudden enlargement or sudden exit loss	1.00	45

A sudden expansion of a pipe will generate more losses than in a gradually expanding pipe. When increasing the diameter of the pipe, velocity will decrease as stated in the continuity equation, but then the pressure will increase (Bernoulli equation). This will generate an adverse pressure gradient that pushes against the flow direction to the smaller pipe, causing turbulence in the corners of the joint (Figure 15). Also this turbulence increases by the difference of velocity between both pipes and it is this turbulence what causes energy losses. (Hamill 2011, 201 - 202).

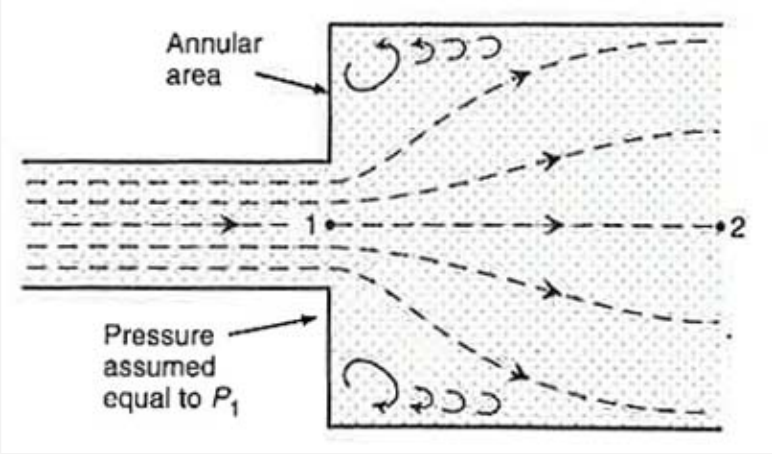

FIGURE 15. A sudden expansion in a pipe full of water (modified from Hamill 2011, 202)

On the other hand, when there is a sudden contraction of the pipe, the head losses are less, because the pressure gradient is no longer adverse to the direction of flow. Nevertheless, the contraction continues still a little after the change of diameter, forming what is called a *vena* contracta (Figure 16), which causes the loss of energy after expanding. This kind of loss can also be prevented by contracting the pipe gradually instead of suddenly. (Hamill 2011, 204).

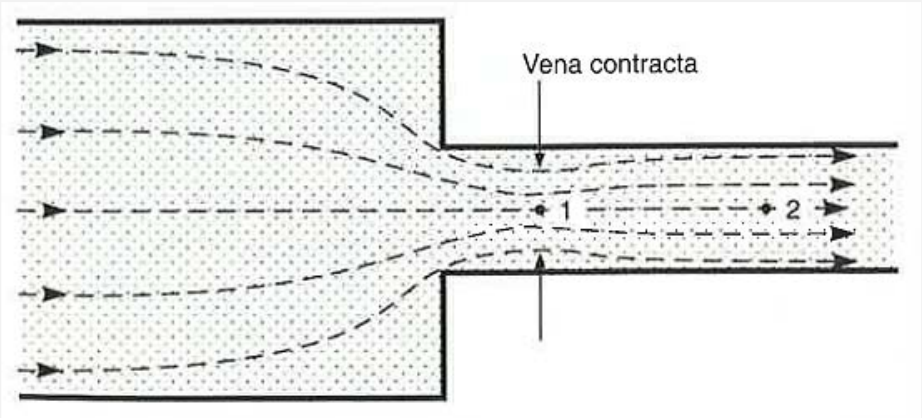

FIGURE 16. Vena contracta after sudden contraction in a pipe (modified from Hamill 2011, 205)

2.4.5 Pumps

Centrifugal pumps are one of the main types of pumps used in water supply as well as in water and wastewater treatment (RIL II 2003, 27). They consist essentially of a casing and a rotating impeller. When water is fed to the center of the impeller, the rotating motion of the impeller causes the water to move radially outwards to the outer casing due to centrifugal force. The water exits tangentially with an increase in pressure and kinetic energy. While water exits, more water is sucked to the center of the impeller, generating a continuous flow. For obtaining higher heads, centrifugal pumps can have more than one impeller, one after another, so that the water is fed to the center of each impeller after leaving the previous one, adding pressure to the water. These pumps are called multi-stage pumps. (Hamill 2011, 398 - 399).

The impellers of centrifugal pumps can be of different size and shape, which results in a wide range of pumps available for obtaining different pressure heads and discharges, as well as the possibility of pumping liquids with solids (Hamill 2011, 399). To avoid clogging in wastewater pumps, there are special impellers that allow the passage of larger particles. The most common types are the single-channel, double-channel, and vortex impellers (Figure 17). (RIL II 2003, 489).

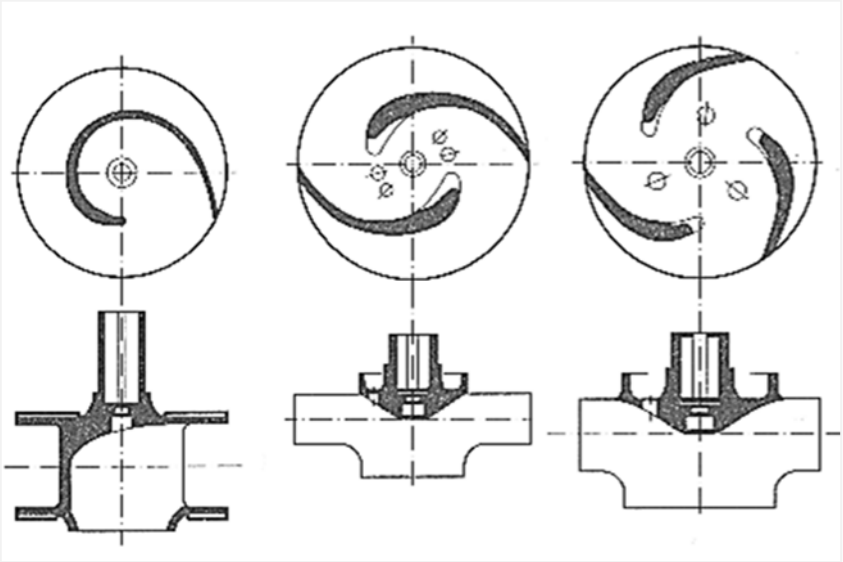

FIGURE 17. Wide passage pump impellers adequate for sewage pumping (RIL II 2003, 489)

Centrifugal pumps can be furtherly classified as radial flow, axial flow, or mixed flow pumps depending on the direction of the flow inside the pump. The flow described at the beginning of this chapter is typical of the radial flow pumps. In axial flow pumps, the water enters and exits the pump in the same direction of the drive shaft of the pump, while mixed flow pumps are a combination of the previous two with water flowing both radially and axially. Of the three types, radial flow pumps are best for obtaining higher heads, followed by mixed flow pumps. Axial flow pumps are best for pumping larger quantities of water at a low head. (RIL II 2003, 27 - 28; Hamill 2011, 398 - 400).

The performance of a certain pump can be described with its so-called performance curves (Figure 18), where the pump's generated head is plotted against the generated discharge (H-Q curve). It is common to include a curve of efficiency (ε) and a curve of power requirement in the same graph, which allows to choose a pump that works at or close to maximum efficiency within the desired range of head and discharge. (Hamill 2011, 400 - 401). The H-Q curve of a pump is called stable if it decreases constantly, so that for every value of head there is only one corresponding value of discharge. On the other hand, the curve is called unstable if it goes up and down or if it is in part horizontal, which means that for a given head, the discharge can vary between two or more values. (RIL II 2003, 29 - 30; Hamill 2011, 406 - 407).

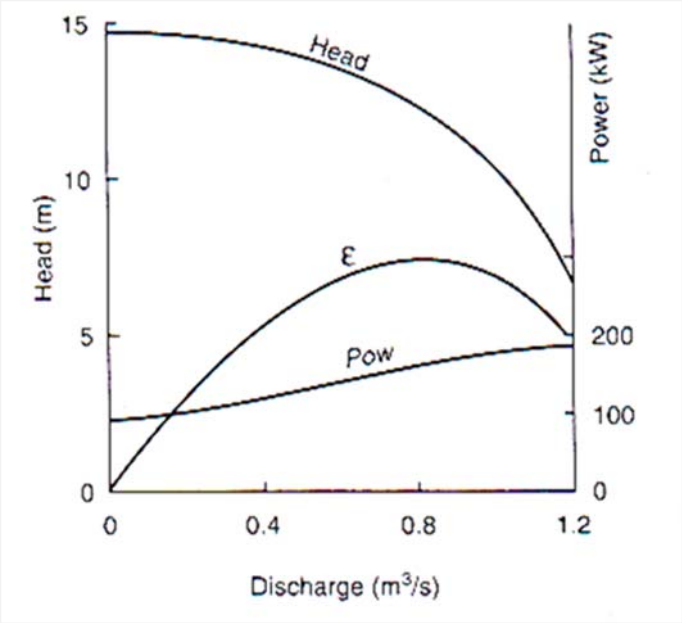

FIGURE 18. Pump performance curves (modified from Hamill 2011, 408)

Other important parameters of a pump are its specific speed N_S and the net positive suction head *NPSH*. The first one is used to describe the speed in rpm at which a discharge of 1 m^3/s is pumped at 1 m head. As a general guide, high head generating radial flow pumps have a N_S value between 10 and 70, mixed flow pumps range between 70 and 170, and for large discharge axial flow pumps the value is above 170. N_S can be calculated with Equation 27. (Hamill 2011, 405).

$$N_S = \frac{N\,Q^{1/2}}{H^{3/4}} \qquad \text{(Eq. 27)}$$

The *NPSH* of the pump represents the minimum head required for the pump to suck the water without cavitating. Cavitation is a phenomenon in which bubbles of gas are formed due to a decrease in pressure below the vapor pressure of the fluid followed by an implosion of the bubbles due to a sudden increase in pressure. Cavitation can physically damage the components of the pump, especially the impeller, as well as affect the performance of the pump, resulting in lower and variating head and discharge. *NPSH* can be calculated with Equation 28, where H_{ATM} is the atmospheric pressure at the pumping site, H_{VAP} is the vapor pressure of the fluid, H_S is the static suction lift, and h_{FS} is the head loss due to friction and minor losses in the suction pipe. (Hamill 2011, 413 - 416).

$$NPSH = H_{ATM} - H_{VAP} - H_S - h_{FS} \qquad \text{(Eq. 28)}$$

The performance of a pump, that is, the head and discharge given by a pump as well as its power requirement, can be modified either by changing the pump's speed *N* or by changing the diameter of the impeller *D*. The relations between these changes and the performance of the pump are known as affinity laws and are given by Equations 29 - 34 in Table 8. (Hamill 2011, 401 - 403).

TABLE 8. Affinity laws for pumps (Hamill 2011, 403)

Variable speed of motor		**Variable diameter of impeller**	
$\frac{Q_1}{N_1} = \frac{Q_2}{N_2}$	(Eq. 29)	$\frac{Q_1}{D_1^3} = \frac{Q_2}{D_2^3}$	(Eq. 32)
$\frac{H_1}{N_1^2} = \frac{H_2}{N_2^2}$	(Eq. 30)	$\frac{H_1}{D_1^2} = \frac{H_2}{D_2^2}$	(Eq. 33)
$\frac{Pow_1}{N_1^3} = \frac{Pow_2}{N_2^3}$	(Eq. 31)	$\frac{Pow_1}{D_1^5} = \frac{Pow_2}{D_2^5}$	(Eq. 34)

In situations when, for example, the discharge requirement fluctuates, or the discharge and head requirement can't be met by a single pump, it is possible to connect two or more pumps in series or in parallel. When connecting the pumps in series, the same water passes through each of the pumps giving a higher head for the same discharge. The resulting head will be the sum of the head given by each of the pumps. This is different from the principle of multi-stage pumps in the fact that the impellers of the multi-stage pump are attached to the same motor and their rotational speed is the same, whereas the connected pumps can have variable speed and operate at different ranges of head and discharge because they are driven by different motors. On the other hand, when connecting the pumps in parallel, the water taken by each pump is gathered into the same pipe after being pumped giving a larger discharge for the same head. (Hamill 2011, 399, 410 - 411).

Besides from the type of pump and its performance within the desired range of head and discharge, some of the things to consider when selecting a pump for a particular task can be mentioned. Both the efficiency and power requirement of the pump are important when considering the cost of running the pump, especially if the pump is continuously working. Also the physical and chemical characteristics of the pumped fluid affect the selection of the pump, for example, selecting the pump material if the fluid is corrosive or the type of impeller if the fluid contains solid particles. It is also important to ensure a *NPSH* high enough to avoid cavitation and to guarantee the efficient performance of the pump. Finally, in some cases, the type of motor and other equipment needed can affect the decision in the selection of the pump. (Hamill 2011, 406 – 407; Karassik, Messina, Cooper & Heald 2001, 11.2 - 11.8).

3 PARTICLE SEPARATION

Solids in water and wastewater are present mainly as particles that need to be removed for health and aesthetic issues. Solids separation from water can be done by many different methods. The methods that are selected for the removal of solids in treatment plants depend on the characteristics of the particles to be removed, like their concentration, density, and size, as well as their attachment to other surfaces, including other particles. Usually more than one method is needed for a satisfactory removal of solids from water. Solids removal methods can be categorized into three: gravity separation, granular media filtration, and membrane filtration. (Benjamin & Lawler 2013, 519 - 521). These methods will be presented in Chapter 4. The particle characteristics of main importance for solids removal will be described in the next chapters, as well as the main mechanisms involved in particle sedimentation.

3.1 Particle characteristics

3.1.1 Particle shape

Particles that are found in water and wastewater have different shapes. Some particles can have a specific shape, like organisms or minerals, but most are particles of very irregular shape, like flocs. Because of this and also for simplicity, particle shape is usually taken as spherical. (Benjamin & Lawler 2013, 551).

For making a correct relation between the actual shape of the particle and its equivalent spherical diameter, the particle's sphericity factor ψ, which is the relation between the surface area of a sphere that has the same volume as the particle and the area of the particle, is considered. Another measure to describe a particle's shape is the shape factor φ, which is the ratio of the area and volume of the particle. Because the sphere is the shape that has the smaller area per volume ratio, the sphere's value of φ is 6 and thus, for any other shape, φ will always be >6 and ψ will always be <1. The relation between these two terms is expressed in Equation 35. (Holdich 2002, 5 - 6; Benjamin & Lawler 2013, 551). Table 9 shows the sphericity values of certain particle shapes.

$$\psi = \frac{6}{\varphi} \qquad \text{(Eq. 35)}$$

TABLE 9. Common particle shape descriptions (modified from Holdich 2002, 6)

Descriptor	ψ	Example
Spherical	1.000	glass beads, calibration latex
Rounded	0.82	water worn solids, atomized drops
Cubic	0.806	sugar, calcite
Angular	0.66	crushed minerals
Flaky	0.54	gypsum, talc
Platelet	0.22	clays, kaolin, graphite

3.1.2 Particle size

Particle size is expressed in terms of diameter, considering that the particle is spherical (Chapter 3.1.1), and its units are expressed in micrometers (μm). Particles in water and wastewater are present in all sizes between a certain range. Usually the lower limit of this range is set arbitrarily or by the measuring device's detection capability. On the other hand, there is always an upper limit that depends on the physical treatments that the water has received. (Benjamin & Lawler 2013, 546). The particles present in water and wastewater can be classified as suspended particles or colloidal particles. Colloidal particles are usually in the size range of 0.001 to 1 μm and cannot be separated by sedimentation processes. (Tchobanoglous et al. 2014, 461 - 462).

There are different methods for measuring the size of the particles in a sample, the most simple being observation through a microscope, although this method is limited and not very practical. More commonly, electronic particle size analyzers are used for this measurement. The measurement in this kind of analyzers is based either in changes in the conductivity of the sample or in the light intensity changes of a laser beam. These changes vary with respect to particle size and produce electrical signals that are sensed by the analyzer, which has to be calibrated beforehand with spheres of different and known sizes. Each of these electrical signals is then related to the size of the particle. (Benjamin & Lawler 2013, 550 - 551; Tchobanoglous et al. 2014, 76 - 78).

The number of particles measured between each size range is the particle size distribution of the sample. Particle size distribution is a function of the diameter and can be presented in terms of number, area, or volume of the particles, and also differentially or cumulatively. Differential distributions in a logarithmic scale are most frequently used. Whether to present the number of particles, their area or their volume in the distribution depends on the particle characteristic that is relevant to the process. For example, for flocculation, surface area is relevant, whereas for sedimentation, it is the volume that matters the most. Also, for different processes, the size ranges and their changes can vary. For example, a decrease in smaller particles in flocculation and a decrease of larger particles in sedimentation. (Benjamin & Lawler 2013, 548 – 549).

3.1.3 Particle charge

There are three main ways a particle's surface becomes positively or negatively charged: isomorphic substitution, chemical reactions, and adsorption. Isomorphic substitution occurs commonly in clays and it is due to the substitution of certain elements in the crystal arrangements of a solid. If the substitute element has a different valence than the replaced original element, the net charge of the solid will change. Chemical reactions at the surface of a particle depend on the water's pH. These reactions happen in solids that have acidic or basic functional groups, like oxides, hydroxides, carbonates, phosphates, and the carboxyl and amino groups of bacteria, for example. With changes in pH, these solids can become protonated or deprotonated and, thus, become positively or negatively

charged. Finally, adsorption on the particle surface is caused by the ions present in water and their interactions with the particles. The adsorption of these ions contributes to the charge of the particle. (Benjamin & Lawler 2013, 522 - 523).

The charge on the surface of particles helps the particle size distribution to remain the same, in other words, makes the particles stable. Thus, for an efficient removal of particles from water, usually the particles have to be destabilized, especially if the particles are colloidal. When two moving particles are either positively or negatively charged, a rejection force between the two will prevent them from collision. Nevertheless, despite being equally charged, if the two particles are close enough, the attractive London-van der Waals forces could bring them together. (Benjamin & Lawler 2013, 521).

The London-van der Waals forces originate from the interaction of two molecules and their polarization. The movement of the electron cloud in a molecule can cause it to be slightly polar at certain times, even if the molecule is nonpolar. When two molecules approach each other, the position of the electron cloud with respect of the other molecule can cause an attraction or rejection between the two of them. For example, if the electron cloud of one molecule faces the positive side of the other molecule, they will experience an attraction. Usually, attractive forces will be longer and more stable than rejection forces and will remain until the molecules separate due to their kinetic energy. (Benjamin & Lawler 2013, 526 -527).

3.1.4 Particle density

The density of particles in water has a wide range, for example, the density of some mineral particles is between 4 and 5 kg/m^3 while flocs and organisms are almost as dense as water. It is the difference between the density of the particles and the density of water that is of main importance for their behavior in water and their further separation, especially in gravity separation. (Benjamin & Lawler 2013, 552). Table 10 shows the densities of some particles commonly encountered in water and wastewater treatment.

TABLE 10. Densities of various particles of interest in water and wastewater treatment (Benjamin & Lawler 2013, 552)

Substance	Density (g/cm^3)
Iron oxide	4.5
Sand	2.65
Clay	2.65
Calcium carbonate	2.4
Flocs of freshly precipitated hydroxides (Al, Mg, Fe)	1.01 - 1.05
Microorganisms (incl. activated sludge)	1.01 - 1.1

3.1.5 Particle destabilization

As noted in Chapters 3.1.2 and 3.1.3, particles that are difficult to settle, like colloids, have to be destabilized in order to remove them by sedimentation processes. The mechanisms for particle destabilization are mainly four: adsorption and charge neutralization, enmeshment in a precipitate (sweep flocculation), adsorption and interparticle bridging, and compression of the diffuse layer. (Benjamin & Lawler 2013, 535).

These mechanisms depend in part on the chemicals (also known as coagulants or flocculants) that are added to the suspension. The type and amount of chemical to be added depends on the suspension properties and has to be determined beforehand with tests (called jar tests). The minimum amount of chemical to destabilize the suspension is known as the critical coagulation concentration (CCC). (Benjamin & Lawler 2013, 535 – 537).

The most commonly used chemicals for destabilization are aluminum and iron salts, and organic polymers. Aluminum is added as aluminum sulfate ($Al_2(SO_4)_3 \cdot xH_2O$) and iron is added either as ferric sulfate ($Fe_2(SO_4)_3$) or ferric chloride ($FeCl_3$). Hydroxides of these metals precipitate during destabilization. Both metal chemistries are quite similar, with the difference that the pH for minimum solubility of $Al(OH)_3$ is about 6.5 while $Fe(OH)_3$ is less soluble and its minimum solubility pH is about 8.0, which makes the latest a more convenient choice in water treatment. The addition of the metal salts reduces alkalinity and pH, so pH is usually monitored and controlled, as well as alkalinity in low alkalinity waters, with the addition of a base. (Benjamin & Lawler 2013, 532 – 533).

The organic polymers that are usual in water and wastewater treatment are the positively charged, low-molecular polydiallyldimethyl ammonium chloride (polyDADMAC) and epichlorohydrin dimethylamine (epi-DMA). The use of these polymers is especially useful in cases where the pH varies quickly in a wide range because their charge density does not change over a large pH range. Organic polymers adsorb to particle surfaces, thus, changing particle characteristics and interactions with each other. (Benjamin & Lawler 2013, 533 - 534).

The mechanism by which aluminum and iron salts, as well as organic polymers act, is the adsorption and charge neutralization mechanism. Colloidal particles in water and wastewater are usually negatively charged, and that is why these kinds of coagulants are the most common. Other chemicals and their mechanisms are ferric chloride in sweep flocculation, synthetic (acrylamide based) polymers in adsorption and interparticle bridging, and inorganic electrolytes (like sodium chloride or calcium chloride) in compression of the diffuse layer. (Benjamin & Lawler 2013, 535 - 541).

3.2 Particle settling

Particles denser than water can settle with the aid of gravity and be, thus, separated by sedimentation processes (gravity separation). Particle sedimentation, or settling, can occur mainly in four different ways: discrete settling, flocculent settling, hindered settling and compression settling (RIL II 2003, 78). The different gravity separation methods commonly used in water treatment are presented in Chapter 4.

3.2.1 Discrete settling

Discrete settling, or Type I sedimentation, occurs in solutions that have low particle concentration and particles that do not tend to flocculate, so the particles can settle individually without interacting with any other particles (RIL II 2003, 76).

The particles of the solution settle influenced only by the gravitational force F_G and the drag force F_D that originates from the particle motion inside a fluid. The mass of the particle considered in the calculation of the gravitational force (Eq. 3) is given by the difference between the particle's and the water's density. When both the gravitational and the drag forces are equal, the particle settles at a steady velocity (Eq. 36).

$$v = \sqrt{\frac{2\,(\rho_p - \rho_w)\,g\,V}{C_D\,\rho_w\,A_p}} \qquad \text{(Eq. 36)}$$

where v is the settling velocity of the particle, ρ_p and ρ_w are the densities of the particle and the water respectively, V is the volume of the particle, C_D is the drag coefficient and A_p is the projected cross-section area of the particle. Considering the particle a sphere of diameter d, Equation 28 can be expressed as in Equation 37. (RIL II 2003, 79 - 80; Tchobanoglous et al. 2014, 346 - 348).

$$v = \sqrt{\frac{4}{3}\frac{(\rho_p - \rho_w)\,g\,d}{C_D\,\rho_w}} \qquad \text{(Eq. 37)}$$

The drag coefficient C_D of spherical particles in the laminar region can be calculated with Equation 38. Substitution of C_D in Equation 37 results in what is known as Stoke's law (Eq. 39). (Tchobanoglous et al. 2014, 347 - 348).

$$C_D = \frac{24}{Re} = \frac{24\,\mu}{\rho\,v\,d} \qquad \text{(Eq. 38)}$$

$$v = \frac{(\rho_p - \rho_w)\,g\,d^2}{18\,\mu} \qquad \text{(Eq. 39)}$$

Although the Stoke's law describes the downwards settling velocity of a particle, if the density of the particle is less than that of the water, the same expression can be used for describing the particle's upwards flotation velocity. Nevertheless, the assumptions made in the Stoke's law, like the spherical shape of the particle and the settling in the laminar region, are conditions that rarely occur in water treatment and, hence, limit its use. (Benjamin & Lawler 2013, 608).

For overcoming these limitations, the value of C_D can be calculated as in Equation 40 for settling in the transitional region and as in Equation 41 for settling in the turbulent region. Also, the shape of the particle can be considered by multiplying Re by the sphericity ψ value of the particle or multiplying C_D by the particle's shape factor φ (Chapter 3.1.1). (Tchobanoglous et al 2014, 347 - 348; RIL II 2003, 79 - 81).

$$C_D = \frac{24}{Re} + \frac{3}{\sqrt{Re}} + 0.34 \qquad \text{(Eq. 40)}$$

$$C_D = 0.4 \qquad \text{(Eq. 41)}$$

3.2.2 Flocculent settling

In flocculent settling (Type II sedimentation), the solution's particle concentration is low but, unlike in discrete settling, the particles in the solution tend to flocculate. The settling velocity of the particles is no longer constant, because when the particles start to stick together, their size and mass increase and, thus, also their settling velocity increases. Flocculation will continue throughout the settling trajectory and so the particles will constantly accelerate. For this reason, particles will settle faster than in discrete settling. (Benjamin & Lawler, 603, 620).

Flocculent settling is strongly influenced by particle concentration, as well as size range and detention time, among others. For this reason, there is not enough theoretical information to predict the flocculation rate or the settling velocity of a certain solution and, therefore, sedimentation tests of the solution have to be made in the laboratory. The results of these tests are usually represented in terms of time, depth, and percentage of solids removal (Figure 19). (Tchobanoglous et al. 2014, 354; RIL II 2003, 82; Droste 1997, 299).

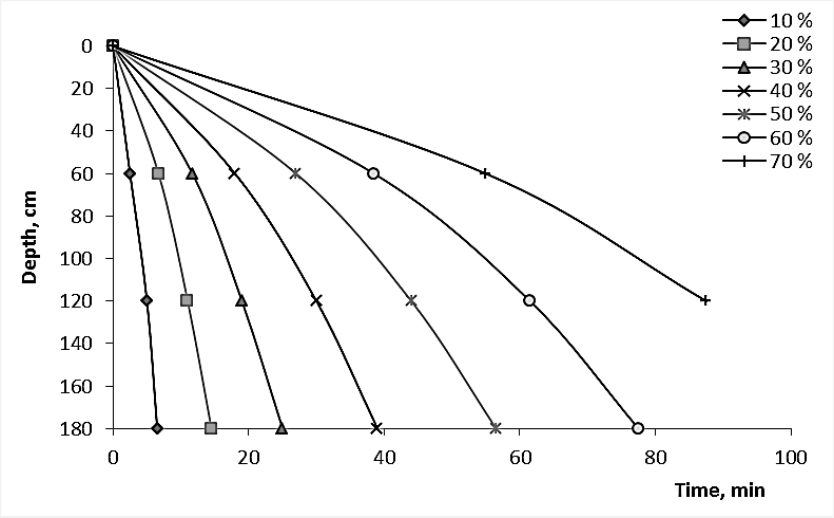

FIGURE 19. Isoconcentration curves (modified from Droste 1997, 302)

3.2.3 Hindered settling

The third type of sedimentation, called hindered or zone settling, occurs in solutions with high solids concentration. As particles settle, water flows upwards between the particles, causing the particles to remain in the same position with respect of each other. Because of this, particles continue to settle as an entity. During sedimentation, a zone of clear liquid starts to form on the top and a settling zone at the bottom, which is the entity of settling particles. (Tchobanoglous et al. 2014, 360; Droste 1997, 308 - 309).

As time passes, the solids at the bottom start to get closer and compress, creating a compression zone. Between the compression zone and the hindered zone becomes visible a transition zone, whose concentration decreases from the compression zone to the hindered zone. Eventually, the solution will reach what is called the critical point, when both the hindered zone and the transition zone disappear (Figure 20). (Tchobanoglous et al. 2014, 360 - 361; RIL 2003, 82).

Although the velocity of sedimentation of a solution in this type of settling also has to be tested, in 1952, Kynch assumed that the settling velocity in each zone depends only on the solids concentration of the zone. From his work is shown that particles in the hindered zone have a constant settling velocity, which starts to decrease in the transition zone, until they finally reach the compression zone. Before the hindered zone sometimes can be present an indefinite zone where flocs are formed. Particles remaining in the clear zone can settle as in discrete or flocculent settling, depending on their characteristics. (Tchobanoglous et al. 2014, 360 - 361; RIL II 2003, 83).

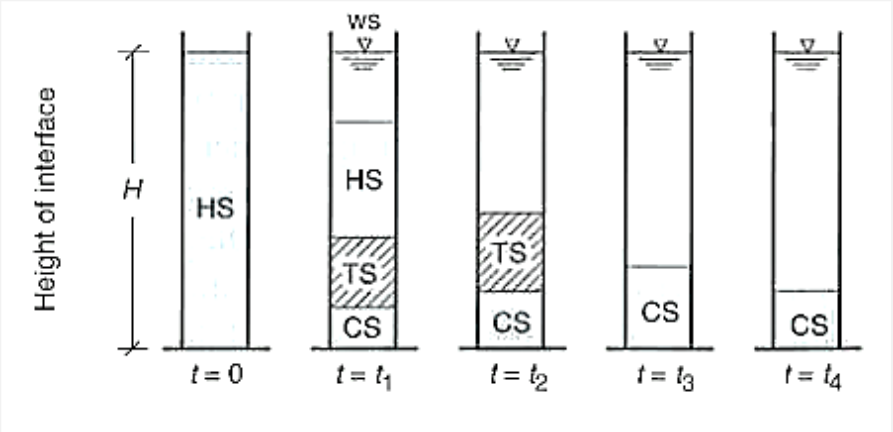

FIGURE 20. Definition sketch for hindered settling (modified from Tchobanoglous et al. 2014, 360)

3.2.4 Compression settling

Finally, compression settling (Type IV sedimentation) occurs after hindered settling in high concentration solutions (Figure 20). As particles settle, their weight pressures against the bottom layer of flocs. Because of this compression, the flocs at the bottom get closer together and lose water. Further compression of this layer can be obtained by stirring, which helps release more water from the flocs. The characteristics of this kind of settling in a particular solution and the effects of stirring have to be determined with sedimentation tests in the laboratory. (Tchobanoglous 2014, 360, 364; RIL II 2003, 82 - 84).

4 SOLID SEPARATION METHODS

4.1 Screening

Screening is one of the first solids removal processes in water and wastewater treatment, although for raw water it is not always required and it is mostly needed in water intake from rivers. In this process, large solids, like trash, paper, leaves and sticks, for example, are separated from the influent water by passing the water through openings of certain, uniform size. The aim of screening is to separate solids that could damage the equipment, like pumps, or affect the efficiency of the whole treatment process. The openings of the screens can have any shape and can be made of bars (bar racks), mesh or plate perforations. The solid material separated by a screen is called screenings. (RIL II 2003, 53 - 54; Tchobanoglous et al. 2014, 310).

Screens can be classified as coarse, medium, and fine screens, depending on the size of their openings. The smaller the size of the openings of the screen is, the more the amount of screenings and need of cleaning. The opening size range for each type is about 40 to 100 mm for coarse screens, 10 to 40 mm for medium screens, and <10 mm for fine screens. In addition to these, there are fine strainers and microscreens with an opening size of about 0.5 to 6 mm for the first and <0.5 mm for the latter. However, these may be used in a different part of the treatment process and may replace other sedimentation processes, since they can also separate some percentage of suspended solids. (RIL II 2003, 53, 502; Tchobanoglous et al. 2014, 310 - 311, 323).

In the design or installation of screens, it is important to consider some aspects, like location, inclination, head loss, opening size, velocity, and screenings disposal, among others. Inclination is usually between 30 to 60 degrees and is important especially in the means of cleaning of the screen, which can be done manually or mechanically. The velocity of the water flow in screening should be over 0.4 m/s but less than 1 m/s. With a lower velocity, the solids could settle before the screen but, with a high velocity, the solids could squeeze through the openings. (Tchobanoglous et al. 2014, 316; RIL II 2003, 53; Droste 1997, 287).

4.1 Sedimentation

Sedimentation is a settleable suspended solids removal process that usually comes as the first process in water and wastewater treatment facilities after grit and coarse solids removal (like screening), although it can also be used as a secondary treatment process after biological treatment. In this process, settleable solids are let to settle in tanks of circular or rectangular shape, known as clarifiers or sedimentation basins, and are then removed by scraping. Floating material (scum) can be removed by skimming of the surface. (Tchobanoglous et al. 2014, 17, 382 - 383).

One of the main parameters for designing a clarifier is to determine its surface loading rate. A rectangular tank of length *l*, width *b*, and depth *h* with a steady flow rate *Q*, has a flow velocity $\vec{v}_f$ equal to:

$$\vec{v}_f = \frac{Q}{A} = \frac{Q}{b\,h} \qquad \text{(Eq. 42)}$$

Supposing ideal settling conditions like no turbulence, no short circuiting, nor remixing of settled particles, as well as uniform distribution of all particle sizes and discrete particle settling (Chapter 3.2.1), the last particle that settles in the tank has a velocity $\vec{v}_s$ with a horizontal component $\vec{v}_x$ and a vertical component $\vec{v}_y$ as shown in Figure 21. The horizontal velocity component is, thus, equal to the velocity of the flow ($\vec{v}_x = \vec{v}_f$). The particle has to settle just before it reaches the opposite side of the tank, so the time it takes it to travel the length of the tank is equal to the time it takes it to travel the depth of the tank (Eq. 43). So the following can be deduced: (Droste 1997,294 - 295; RIL II 2003, 86 - 87).

$$t = \frac{l}{\vec{v}_x} = \frac{h}{\vec{v}_y} \qquad \text{(Eq. 43)}$$

$$\vec{v}_y = \frac{Q}{l\,b} = \vec{v}_c \qquad \text{(Eq. 44)}$$

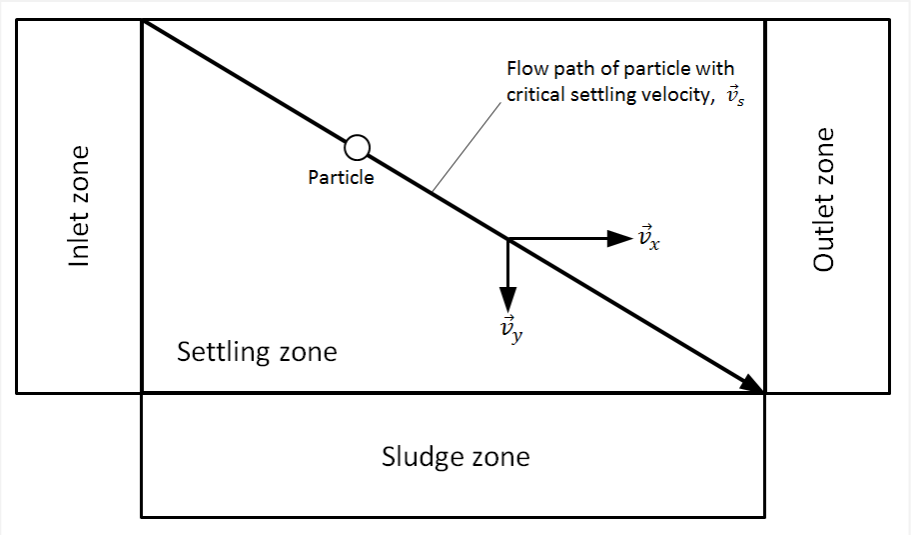

FIGURE 21. Definition sketch for the analysis of ideal discrete particle settling (modified from Tchobanoglous 2014, 351)

All the particles with a settling velocity equal to or greater than this critical velocity $\vec{v}_c$ (the surface loading rate or *overflow rate*, usually given in $m^3/m^2/d$) will settle in the tank. The particles with a lower settling velocity $\vec{v}$ will be proportionally removed according to Equation 45, where X is the fraction of particles removed. (Tchobanoglous et al. 2014, 350 - 351).

$$X = \frac{\vec{v}}{\vec{v}_c} \qquad \text{(Eq. 45)}$$

As shown in Eq. 44, the surface loading rate and particle removal in the tank depend solely on the flow rate and the surface area of the tank and not on its depth, regardless of the shape of the tank,

that is, the same applies for a tank of circular shape. Nevertheless, even if the surface rate is a measurement parameter widely used for clarifier design, the assumptions made for its calculation are not met all the time. In other words, due to factors like turbulence, particle shape, uneven particle and flow distribution, among others, not all the particles with a velocity $\vec{v}_c$ will be removed. (RIL II 2003, 87 - 88; Tchobanoglous et al. 2014, 393).

Since theoretically only the surface area is relevant to particle removal, there are enhanced clarifiers (known also as lamella clarifiers) that have stacked inclined plates or tubes. The extra surface area provided by these allows a more efficient particle removal within a smaller space. The ideal inclination of the plates is between 45° and 60°, which allows the plates to be self-cleaning. Smaller angles can be used but settled particles would accumulate on the plate and require cleaning. Lamella clarifiers can be classified as countercurrent, cocurrent and cross-flow clarifiers, depending on the direction of the flow and the direction of the settled particles (Figure 22). (Tchobanoglous et al. 2014, 356 - 357; Droste 1997, 307).

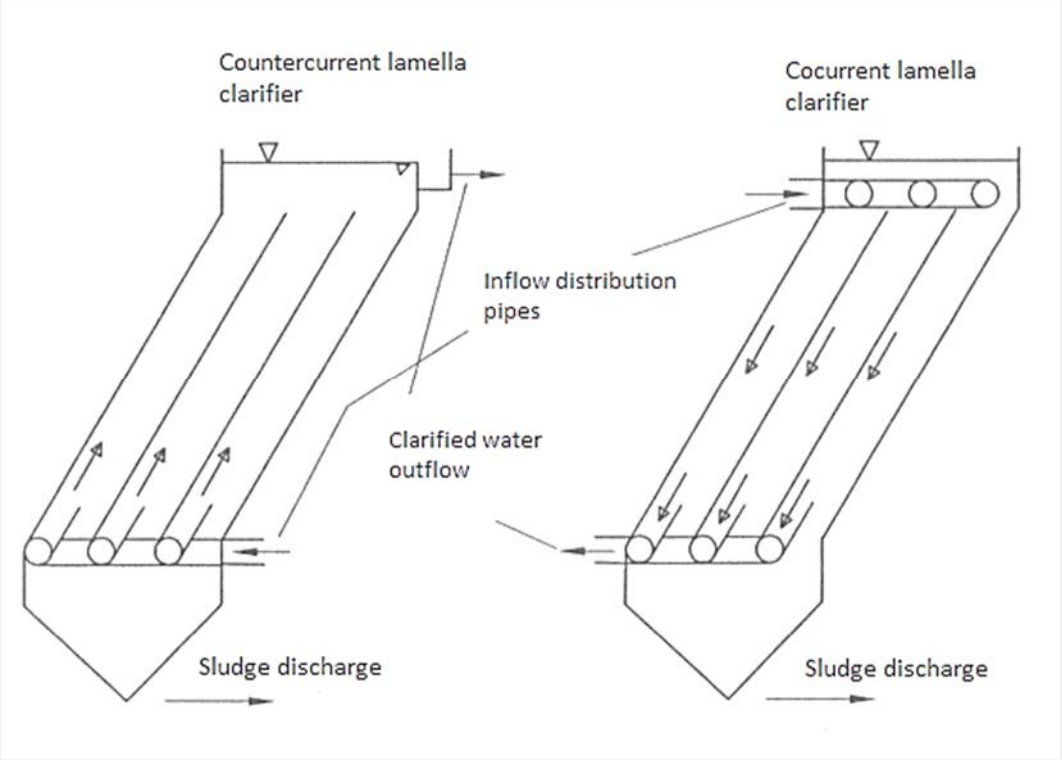

FIGURE 22. Countercurrent and cocurrent lamella plate clarifiers (modified from RIL II 2003, 85)

Other considerations for the design of clarifiers are detention time, and horizontal velocity to avoid resuspension of particles, as well as controlling turbulence and short circuiting, which can occur because of temperature differences between the inflow and the water in the tank, wind or inadequate tank design. (Tchobanoglous et al. 2014, 392 - 395; RIL II 2003, 92).

4.2 Flotation

Flotation is a separation process in which small air or other gas bubbles are released in the water to remove solids and liquids. The bubbles, with a diameter size of around 40 to 70 µm, attach to the

surface of the particles (or flocs of particles) increasing their buoyancy and making them float, even if the particles are denser than water. The floating particles are then removed by skimming of the surface of the water. The rise of particles less dense than water, like oil and grease, is also known as natural flotation, although air flotation can be used to make them rise faster. Destabilization of the particles by coagulation (Chapter 3.1.5) is also used along with this process to improve the attachment of the bubbles to the particles. (RIL II 2003 97; Tchobanoglous et al. 2014, 403 - 406).

There are two main processes by which the bubbles in the water are formed. One way is to make the water become supersaturated with air by saturating it under pressure and then releasing the pressure to atmospheric level. This process is known as dissolved-air flotation (DAF) and it is the mostly used in municipal wastewater treatment facilities. However, is not always convenient to pressurize all the incoming flow, especially in large facilities, so it is only part of the treated water that is returned to the process, pressurized, and saturated with air. The second way is to mix the air into the water at atmospheric pressure with a rotating impeller, which is known as dispersed-air or induced-air flotation. This process is used mostly for removal of oils and suspended solids of industrial wastewaters. (Tchobanoglous et al. 2014, 404 - 405).

For the design of DAF systems, one of the most important parameters to determine is the volume of air and mass of solids ratio (A/S). This parameter is a function of the solubility of air, the operating pressure and the solids concentration and it is obtained experimentally with laboratory tests of the actual solution to be treated. Other parameters that affect the clarification process are the solids loading rate and the rise velocity of the particles. (Tchobanoglous et al. 2014, 406 - 407).

4.3 Filtration

Filtration is a process by which small suspended or colloidal particles are removed from water, which is why filtration is often used as a complement after sedimentation or flotation (Droste 1997, 229). Filtration can be divided as depth filtration or surface filtration. In the first one, filtration occurs by passing the suspension through a whole layer of granular media, while in the latest, the solution is passed through a thin, porous material. A third type of filtration is membrane filtration, which differs from surface filtration by the size of the openings of the filter material, which are 5 – 30 µm for surface filtration and <2 µm for membrane filtration. (Tchobanoglous et al. 2014, 1129, 1171).

Surface filtration can be used instead of granular filtration to remove suspended solids and algae or as a pretreatment before membrane filtration. The filters in this type of filtration have openings of 5 to 30 µm and can be classified as two-dimensional (synthetic or woven metal fabrics) or three-dimensional (like polyester needle felt cloth). Most commonly, surface filtration is accomplished by several rotating metal disks on which the filter material is attached. (Tchobanoglous et al. 2014, 1171 - 1175).

On the other hand, membrane filtration can be furtherly classified as microfiltration, ultrafiltration, nanofiltration, reverse osmosis, and electrodialysis, depending on the size of the pores of the filter

(membrane). These mechanisms are used to separate, among others, colloidal material, cells and microorganisms, and even dissolved molecules (with reverse osmosis and electrodialysis). The membranes can be tubular, fine hollow fibers, or flat sheets made of polymers like polypropylene, polysulfone and aromatic polyamide, cellulose acetate, or ceramic, among others. These membranes are assembled in modules, in which the solution can flow inside-in or outside-out usually with the help of pressure or vacuum. (Tchobanoglous et al. 2014, 1181 - 1186; RIL II 2003, 126 - 127).

In depth filtration, the filter or granular media is typically a layer of sand, although some other materials (like anthracite) or a combination of them can be used. A supporting layer of gravel can be at the bottom of the filter separating the filter and the underdrain. Usually, the suspension enters on the top part of the filter and comes out from the bottom. The filter has to be cleaned regularly to avoid an excessive increase of the head loss or of the turbidity of the water. Cleaning of the filter is done by backwashing, that is, by letting clean water flow upward from the underdrain to the top of the filter. (Tchobanoglous et al. 2014, 1129 - 1134). Figure 23 shows the general principles of a granular media filtration process.

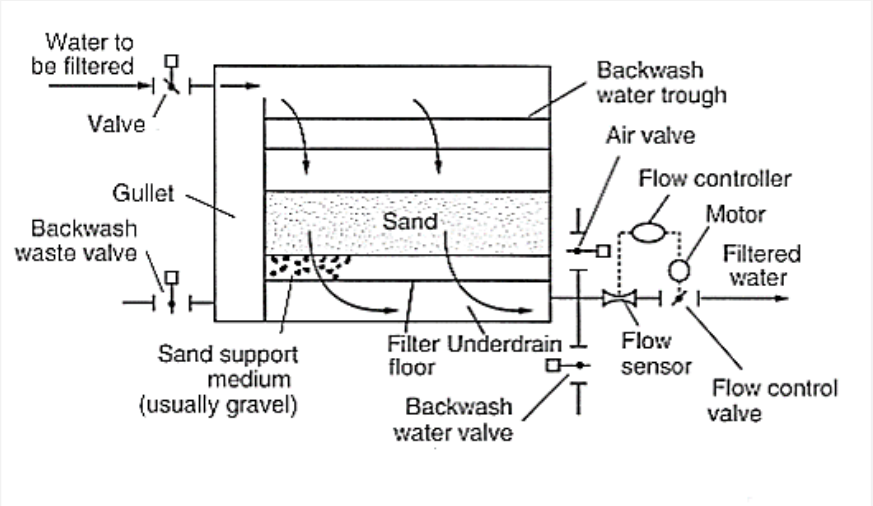

FIGURE 23. General features of a conventional rapid granular medium depth filter (modified from Tchobanoglous et al. 2014, 1130)

There are several mechanisms for a particle to be removed by the grains of the filter. Some of these mechanisms are straining, sedimentation, interception, adhesion and diffusion, among others (Figure 24). Straining is the main mechanism by which particles are removed from water and happens when the space between grains of the filter is smaller than the size of the particle. Sedimentation occurs when particles settle on top of the grains separating from the streamlines, while interception happens to particles that follow the streamlines, but get into contact with the surface of the grains. Adhesion also happens as particles pass by but they can detach and go deeper until there is not enough force to separate them from the grain surface. (Tchobanoglous et al. 2014, 1132 - 1133).

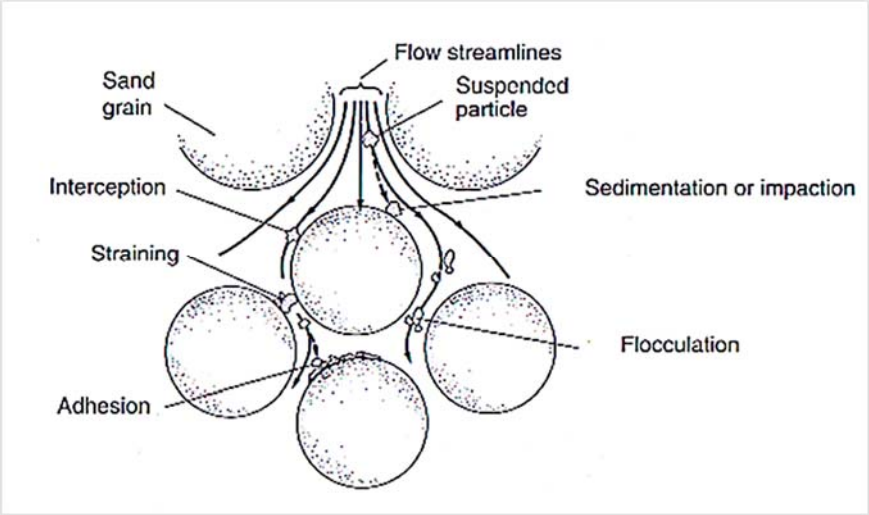

FIGURE 24. Mechanisms for removal of suspended particulate matter within a granular filter (modified from Tchobanoglous et al. 2014, 1133)

Some of the considerations for the design of depth filtration systems are the filter and filter-bed characteristics, allowed head loss, backwash mechanism and amount of water required for backwashing, and filtration rate. The filter grain size and size distribution are of main importance since they not only affect the effective removal of the particles but also the head loss, which are also affected by the filter-bed depth and porosity. (Tchobanoglous et al. 2014, 1130 - 1131, 1162).

4.4 Centrifugation

As seen in Chapter 2.2.2, centrifugal force causes an outward throw when an object moves in a circular pattern, which is the principle by which centrifuges and cyclones work. Centrifugation is another way to speed up the settling of a particle, since the particles are subject to a centrifugal acceleration that can be many times greater than the acceleration caused by gravity.

4.4.1 Centrifuges

The centrifuges used in water and wastewater treatment facilities are used to thicken or to dewater sludge. They consist of a cylinder that rotates at high speed and that ends with a conical section. Inside this cylinder is a screw that rotates at a slightly different speed (Figure 25). The solution is fed in the middle of the cylinder, where the centrifugal force produced by the rotation of the cylinder causes the solid, denser particles to move towards the wall of the cylinder. The separated solids are then removed by the action of the internal screw, which scrapes the solids and conducts them to the end of the conical part to be discharged. (RIL II 2003, 104; Droste 1997, 732).

Depending on the direction of the removed solids with respect to the feed flow, centrifuges can be countercurrent or cocurrent (Figure 25). In the first, the solution is fed axially at the beginning of the conical part and solids are removed from the end of the conical part, moving against the direction of the solution. This is the kind of centrifuge most common in water treatment, since it is not affected

by variations in the feed rate and can also handle solutions with high concentrations of solids. In the cocurrent centrifuges, the direction of the solution and the solids removal is the same. This allows a flow with less turbulence but, on the other hand, they are prone to wearing damages and maintenance problems. This kind of centrifuges is used to treat solutions with a low concentration of solids. (Tchobanoglous et al. 2014, 1571 – 1573; RIL II 2003, 105).

Besides the type of centrifuge and the physical and chemical characteristics of the water and the particles, some of the considerations for the design of centrifugal processes are the feed flowrate, depth of the settling zone, and rotational speed of the cylinder and of the internal screw. The rotational speed of the cylinder of the centrifuge is usually between 200 and 8000 rpm with G values ranging from 800 to 4000, much greater than the value of *g*. (Tchobanoglous et al. 2014, 1573; Droste 1997, 732; RIL II 2003, 105).

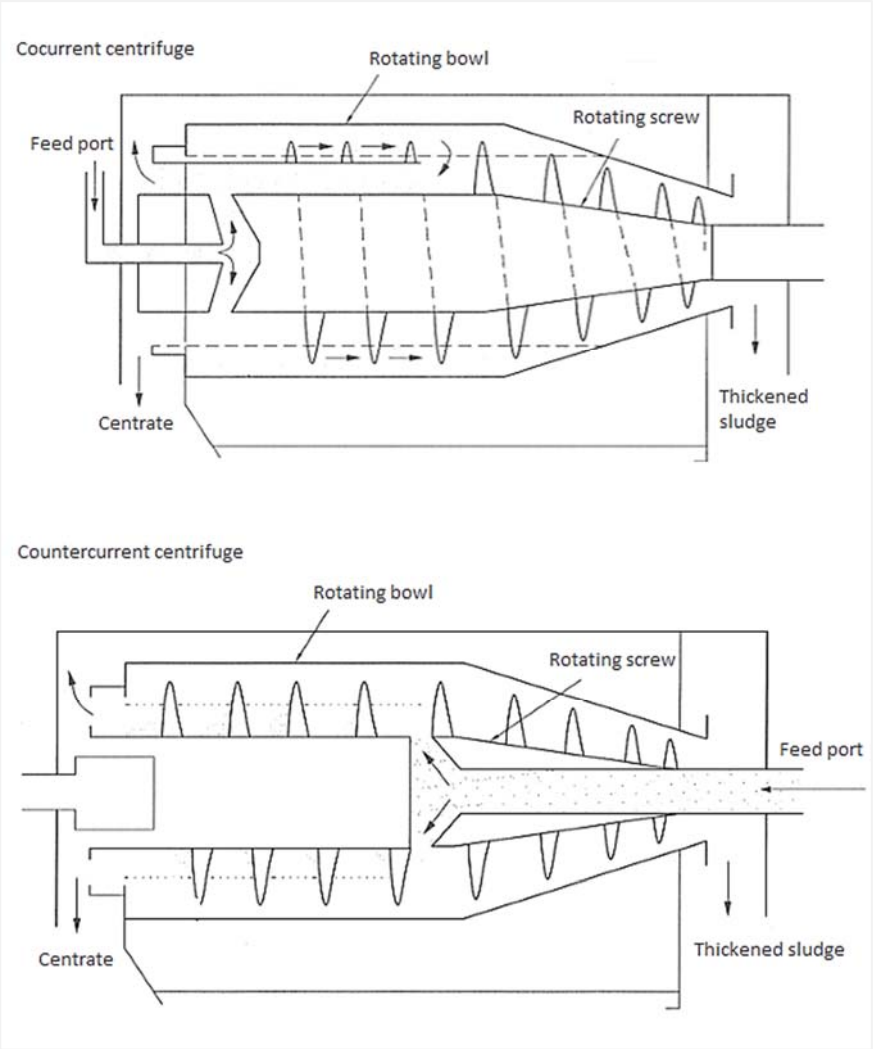

FIGURE 25. Cocurrent and countercurrent centrifuges (modified from RIL II 2003, 104)

It is also important to consider the location of the centrifuge since, even though the area requirement is much smaller compared to other methods, the space has to be well founded and soundproofed due to the vibrations and noise caused by the centrifuge. Also, the maintenance and running costs of the centrifuge can be high and have to be taken into account, which is why this method is mostly used in

large facilities, where the space is reduced, or with sludge difficult to treat by other methods. (Tchobanoglous et al. 2014, 1493, 1573).

4.4.2 Hydrocyclones

The hydrocyclone is also a centrifugal separation device with no moving parts. In this method, centrifugal acceleration in caused by feeding the suspension tangentially at a high speed into a cylinder, as opposed to rotating the cylinder like in centrifuges. The hydrocyclone consists mainly of a cylinder with a conical end, a vortex finder tube at the top, and an apex cone at the bottom (Figure 26). The inlet to the cylinder can be tangential or spiral-shaped. (Peker & Helvaci 2008, 448 - 449; Holdich 2002, 80).

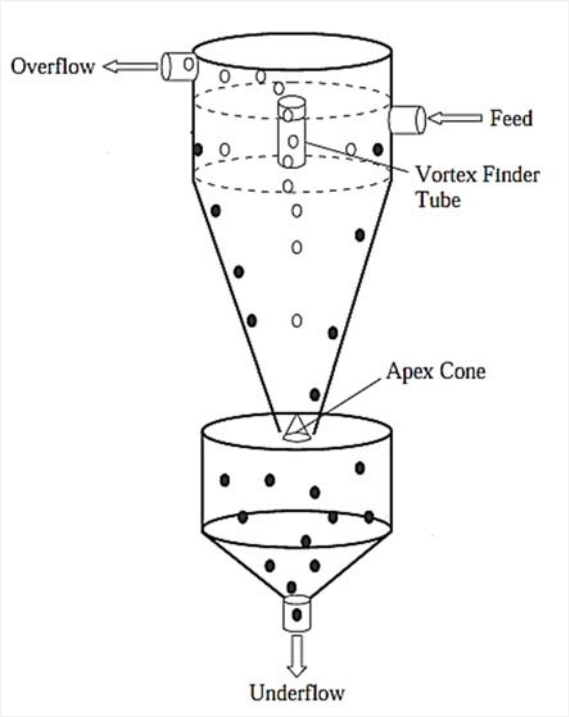

FIGURE 26. Functional parts of a hydrocyclone (modified from Peker & Helvaci 2008, 449)

When the solution is fed tangentially into the cylindrical part of the hydrocyclone, the larger, heavier particles move radially towards the wall of the cylinder due to the centrifugal force. This part of the hydrocyclone functions as a classifier. The particles lose their momentum when they hit the walls of the conical part at bottom and descend in the primary vortex to the underflow with the help of gravity. The particles that did not crash continue moving with the flow in the secondary vortex towards the overflow at the top of the cyclone. (Peker & Helvaci 2008, 448; Holdich 2002, 80).

The tangential, radial, and axial velocities inside the hydrocyclone are of great importance. Tangential velocity, which can be up to 20 m/s, is responsible for creating the centrifugal acceleration. Radial velocity is not as great in magnitude (< 0.1 m/s) but it is important to know whether it is the velocity of the solid (outward flow) or of the liquid (inward flow). Both the centrifugal and the drag forces cause the particles to move radially. Finally, there is axial velocity both downwards to the underflow

with the larger particles and upwards to the overflow with the lighter particles. (Holdich 2002, 80 - 81).

Axial velocity is important to the definition of the cut size (x_{50}) of the hydrocyclone. Since there is axial velocity downwards and also upwards, there must be a region at a certain radial distance where there is no axial velocity. The particles that move within this region have the same chance to go to the underflow or to the overflow and their size is known as the cut size of the hydrocyclone. Most of the particles that are larger than the cut size will leave in the underflow, while most of the particles smaller than the cut size will leave in the overflow. The proportion of larger particles that report to the overflow and of the smaller particles that report to the underflow is given by the grade efficiency and reduced grade efficiency curves, calculated with Equation 46 and 47. (Holdich 2002, 80 - 83).

$$E = \frac{\dot{m}_u}{\dot{m}_f} \qquad \text{(Eq. 46)}$$

$$E' = \frac{E - R_f}{1 - R_f} \qquad \text{(Eq. 47)}$$

where E is the grade efficiency of the hydrocyclone, $\dot{m}_u$ is the mass flow in size grade in underflow, $\dot{m}_f$ is the mass flow size grade in feed, E' is the reduced grade efficiency, and R_f is the volumetric flow speed or recovery, which is the relation of volumetric flow in the underflow and the feed.

The separation efficiency of the hydrocyclone is a function of its dimensions, the pressure drop, and the characteristics of the solution. Factors that reduce separation efficiency include the turbulence of the flow, short circuiting from the feed to the vortex finder, and mixing in the apex cone area. (Peker & Helvaci 2008, 450, 456).

5 SAOXFUGE PROTOTYPES

SansOx Limited has designed and patented a centrifugal solids separator device called SaoxFuge. SaoxFuge's first prototype is a spiral-shaped pipe with two outlets of different size (Figure 27). The smaller outlet pipe is an expansion of the main pipe and its purpose is to remove the separated solids from the main flow, which comes out from the bigger outlet pipe. The solution that enters the SaoxFuge is subject to a centrifugal acceleration caused by the circular flow pattern of the spiral pipe.

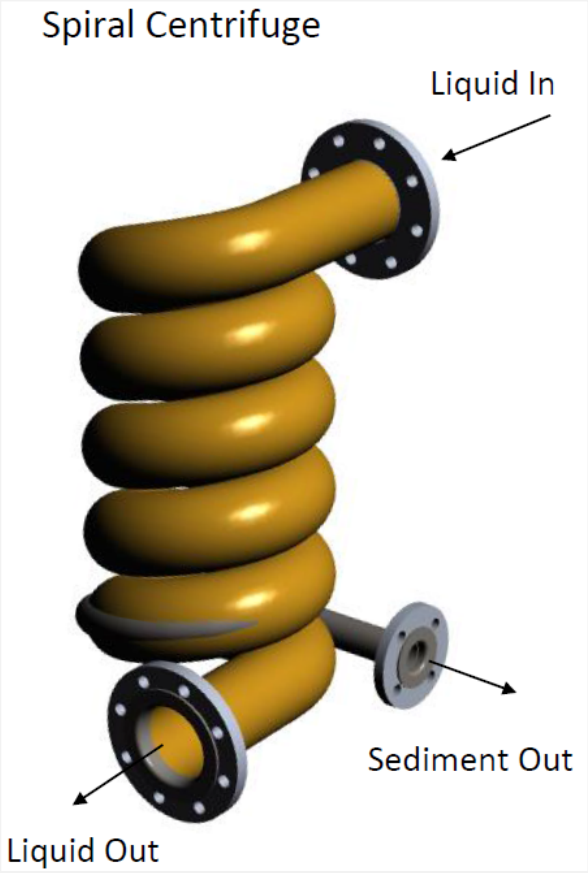

FIGURE 27. SansOx solutions. Spiral centrifuge (SansOx 2015)

A second prototype consists of a cylinder with an internal screw. Water is fed to the cylinder tangentially and flows in a circular pattern due to the screw. A rectangular opening on the side of the cylinder removes the separated solids by skimming, as opposed to the expansion of the previous prototype. The first version of this prototype, which was tested in the summer of 2015, had a clean water exit that was located radially. The second and third versions have this exit located at the bottom of the cylinder, after a conical area, which reminds of the shape of a cyclone (Figure 28).

The performance of all of these prototypes depends strongly on the flow velocity, the position of the prototype, and the characteristics of the solution. Flow velocity is responsible for the magnitude of the centrifugal acceleration, so it is important that it is high enough to generate acceleration greater than that of gravity. Nevertheless, with increased velocity there is also increased turbulence.

The position of the prototype, especially the spiral-shaped prototype, will affect the place in the pipe where the separated solids accumulate. If the area of accumulation and the opening of the solids removal pipe do not meet, there will be no solids removal.

Finally, the characteristics of the solution are important, especially the particle density and size. Small colloidal particles whose density is close to that of water and that cannot be separated by sedimentation will still be difficult to separate during the short time they are inside the SaoxFuge, even if the centrifugal acceleration is significantly higher than gravity.

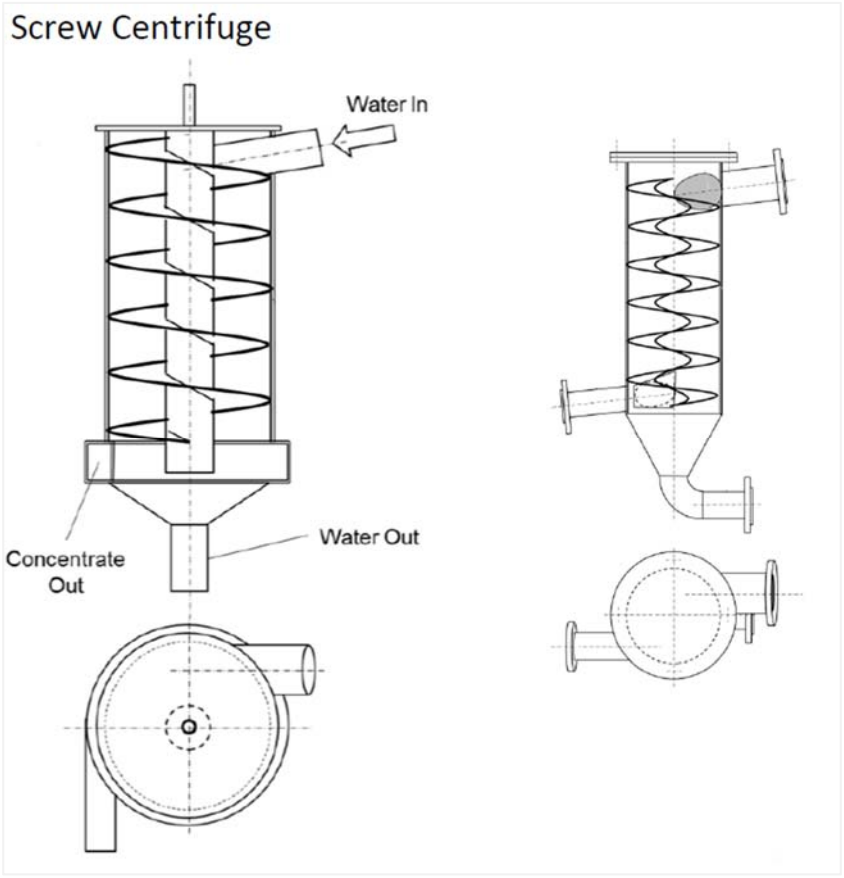

FIGURE 28. SansOx solutions. Screw centrifuge (modified from SansOx 2015)

The discharge required to obtain with the SaoxFuge spiral prototype a centrifugal acceleration equivalent to that of a solid bowl centrifuge (Chapter 4.4.1), with a value of 800 G's, can be calculated as follows, supposing that the dimensions of the prototype are the ones shown in Appendix 1.

$$a = 800 * 9.81 \frac{m}{s^2} = 7848 \frac{m}{s^2}$$

The velocity required for obtaining the previously calculated centrifugal acceleration can be calculated with Equation 5, considering the mean diameter of the spiral centrifuge of 0.230 m.

$$v = \sqrt{7848 \frac{m}{s^2} * 0.115\ m} \approx 30 \frac{m}{s}$$

The discharge required to obtain this tangential velocity is then calculated by multiplying the velocity by the cross-sectional area of the pipe. The velocity of the flow has been calculated taking into consideration the lead angle of the spiral, which is approximately 9.4°.

$$Q = 30\ \frac{m}{s} * \pi * \left(\frac{0.1103}{2}\ m\right)^2 \approx 0.29\ \frac{m^3}{s}$$

The discharge of nearly 300 liters per second makes it quite challenging for the spiral prototype to generate a centrifugal acceleration slightly similar to that of a solid bowl centrifuge. The challenge is not only because of the costs of purchasing and especially running the required pump, but also because of the volume of water needed to be treated, which would be only found in remarkably large water treatment facilities.

If it would be aimed to avoid the turbulent flow, the velocity needed for the flow to be laminar in the spiral prototype can be calculated with Equation 13, with a Reynolds number value of 2000.

$$v = \frac{2000 * 1.518 * 10^{-3}\ \frac{Ns}{m^2}}{1000\ \frac{kg}{m^3} *\ 0.1103\ m} \approx 0.028\ \frac{m}{s}$$

This velocity equals a flow rate of approximately 0.26 l/s and a centrifugal acceleration of 6.6 * 10^{-3} m/s^2, which is much lower than that of gravity. Thus, the flow cannot be laminar if it is aimed to generate a centrifugal acceleration that is greater than or even equal to gravity.

Considering the discrete settling of a particle whose density is 2000 kg/m^3 and whose diameter is 100 µm in water at 4 °C, the settling velocity of the particle can be calculated with the Stokes law (Equation 36) as follows:

$$v = \frac{(2000 - 1000)\ \frac{kg}{m^3} *\ 9.81\ \frac{m}{s^2}\ * 10 * 10^{-9}\ m^2}{18\ * 1.518 *\ 10^{-3}\ \frac{Ns}{m^2}} \approx 0.004\ \frac{m}{s}$$

The above mentioned characteristics of the particle and the conditions of the flow were set arbitrarily but considering a density that is about two times greater than the water density and a size that is big enough to be considered for removal with sedimentation processes. As mentioned in Chapter 3.2.1, Stoke's law considers the particle spherical in shape and the settling occurs in the laminar region.

To increase the settling velocity of this particle ten times with centrifugal force, an acceleration of 10 G's is needed. To generate this acceleration in the spiral prototype, it would require a discharge of approximately 33 l/s, as previously calculated. This flow rate, although still large, is more realistic and accomplishable.

Rounding the discharge value to 30 l/s, which would generate about 8.5 G's, the Reynolds number value and the head losses of the flow are calculated.

$$Re = \frac{1000\ \frac{kg}{m^3} * \ 3.14\ \frac{m}{s} * \ 0.1103\ m}{1.518 * \ 10^{-3}\ \frac{Ns}{m^2}} \approx 2.3 * 10^5$$

Since the Reynolds number is considerably greater than 4000, the flow is obviously turbulent and head loss by friction can be calculated using the Darcy-Weisbach equation (Eq. 21) with a friction factor taken from the Moody diagram using a roughness value *k* of 0.1 mm (value for a new welded acid-proof steel pipe from RIL I 2003, 142). The length of the pipe in the spiral has been estimated using the data in Appendix 1.

$$h_F = \frac{0.02 * 4\ m * \left(3.14\ \frac{m}{s}\right)^2}{2 * 9.81\ \frac{m}{s^2} * 0.1103\ m} \approx 0.37\ m$$

The minor losses in the spiral are caused by the continuous bend of the pipe. Each turn of the spiral equals four 90° bends, amounting to 20 bends in total. The ratio of the radius of the spiral and the diameter of the pipe is just about 1, so the resistance coefficient value, taken from Table 7, is 0.40 and the minor losses can be calculated with Equation 26.

$$h_L = 20\left(0.40 * \frac{\left(3.14\ \frac{m}{s}\right)^2}{2 * 9.81\ \frac{m}{s^2}}\right) \approx 4.0\ m$$

The total head loss at a flow rate of 30 l/s would be about 4.4 m and it has to be taken into consideration when choosing a pump.

Assuming that settling occurs in the turbulent zone, the particle is not spherical (taking $\psi = 0.5$), and the main force acting on the particle is the centrifugal force and not the gravitational force, it is possible to recalculate the settling velocity of the particle using Equation 36. The drag coefficient in the turbulent region is calculated by multiplying the value given by Equation 41 by the shape factor of the particle, calculated with Equation 35.

$$C_D = 0.4 * \frac{6}{\psi} = 4.8$$

$$v = \sqrt{\frac{2 * (2000 - 1000)\frac{kg}{m^3} * \ 83.42\ \frac{m}{s^2} * 5.236 * 10^{-13}\ m^3}{4.8 * 1000\ \frac{kg}{m^3} * 7.85 * 10^{-9}\ m^2}} \approx 0.048\ \frac{m}{s}$$

Even considering the turbulent zone and the non-spherical shape of the particle, it is possible to increase considerably the settling velocity of the particle, as long as the centrifugal force is greater than gravity and the particle is denser than water.

Estimating the volume of water that can be held inside the prototype as 40 l, the time it would take to a particle from the entrance to the exit of the prototype (the retention time) can be calculated by dividing the volume of the prototype by the discharge.

$$t = \frac{0.04\ m^3}{0.03\ \frac{m^3}{s}} \approx 1.3\ s$$

Based on the previously calculated velocity of the particle, the particle would have traveled in this time about 62 mm, which is more than the inner radius of the pipe. This indicates that the particle can travel to the outer wall of the pipe during the time it is inside the prototype.

The direction of the particle $\vec{a}_p$ is the resultant determined by the directions of both the centrifugal acceleration $\vec{a}_C$ and gravity $\vec{g}$. The direction of the drag is opposite to this resultant, so the direction of the velocity of the particle will determine the direction of the drag.

Supposing that the spiral prototype's centerline is completely vertical, the direction of the centrifugal acceleration is horizontal, perpendicular to the centerline, and the direction of gravity is parallel to the centerline. By adding these two vectors, it is possible to determine the magnitude and direction of the acceleration that the particles in the solution will be subject to. Figure 29 shows the graphical addition of the vectors. The magnitude of the resultant vector is calculated as follows:

$$\vec{a}_p = \sqrt{\vec{a}_C{}^2 + \vec{g}^2} = \sqrt{83.42^2 + 9.81^2}\ \frac{m}{s^2} \approx 83.99\ \frac{m}{s^2}$$

This value, although being greater than the centrifugal acceleration, is quickly reduced by the opposing drag, which is why the previously calculated settling velocity of the particle is quite slow. Next, the direction of the acceleration is calculated.

$$\theta = \tan^{-1}\left(\frac{9.81\ \frac{m}{s^2}}{83.42\ \frac{m}{s^2}}\right) \approx 6.71°$$

The opening of the smaller pipe of the prototype is located 15° above and 15° below the horizontal centerline of the pipe. The angle calculated before lies in the opening area, which indicates that separation is possible. At this centrifugal acceleration value, gravity and the position of the prototype do not significantly affect the angle of the resultant. Nevertheless, at lower velocities (smaller centrifugal acceleration), gravity is a more important factor and the direction of the resultant can point towards the area under the opening of the pipe and, thus, particles would continue in the main flow.

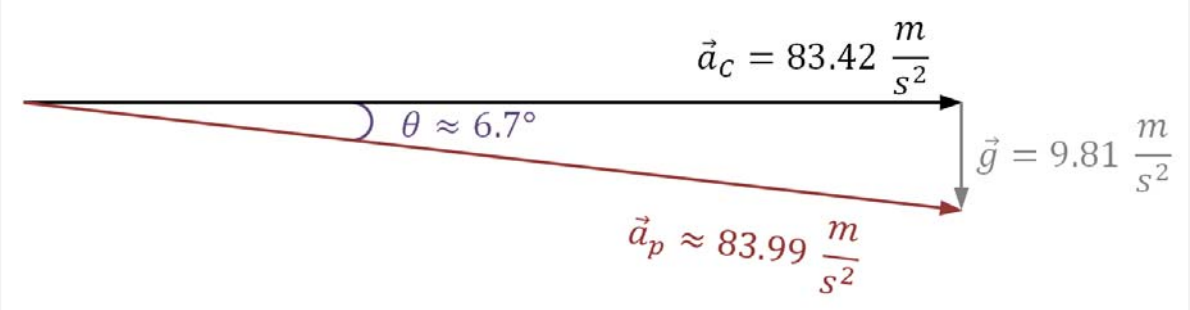

FIGURE 29. Acceleration vectors addition

In summary, separation with the SaoxFuge spiral prototype is possible in theory, as long as the solid particles are denser than water and the velocity of the flow generates a centrifugal acceleration sufficiently higher than gravity. The flow required for this would have to be turbulent, since for the flow to be laminar, the velocity would not generate a centrifugal acceleration high enough. Also, the increase in the velocity of the particles will increase the opposing drag to which the particles will be subject.

The head losses within the prototype also increase with increasing the flow velocity. When choosing a pump, it is important to consider these losses in the head generated by the pump, taken from the pump's performance curve. If the head given by the pump at the desired discharge is lower than the losses, a decrease in velocity will occur, unless there is a sufficient difference in potential energy.

Finally, for the separated particles to be removed from the main flow, it is important that the direction of the particles lies inside the opening area in the main pipe and that they can travel towards this area during the retention time. Since the opening is located between 15° above and 15° below the horizontal centerline of the pipe, the centrifugal acceleration has to be high enough to overcome the downwards direction caused by gravity or by the position of the prototype.

6 REVIEW OF THE PREVIOUS TESTS OF THE PROTOTYPES

The first tests of the SaoxFuge spiral prototype were made during the summer of 2014. The tests were joint tests of both the SaoxFuge and SansOx's OxTube, which is an aeration device. The devices were tested in four different locations with water of different characteristics in each one. These included testing with municipal wastewater, industrial wastewater from Valio's cheese factory in Lapinlahti and Powerflute's Savon Sellu paperboard mill, a propylene glycol and water mix used as antifreeze on the airplanes at Kuopio airport, and, finally, groundwater with a high concentration of iron and manganese.

The second tests of the spiral prototype and first tests of the screw prototype were carried out in the summer of 2015 at Yara Finland Siilinjärvi site's concentration plant, where the main product is apatite, a source of phosphorus for use in fertilizers. These tests were made as part of the KaivosVV project, a project aiming to improve the technologies for mine water treatment. This project was coordinated by the Geological Survey of Finland (GTK) and done in cooperation with Savonia University of Applied Sciences, the University of Eastern Finland (UEF), and the National Institute for Health and Welfare (THL). In this thesis, only the SaoxFuge 2015 tests will be reviewed.

The water used for the 2015 tests was the overflow of the apatite clarifier of the concentration plant. Initially, also the water from the intermediate clarifier at the site was intended to be used in the tests, but because of technical difficulties only the apatite clarifier overflow was used. The site's manager Keränen (2015) gave general information about the clarifiers before the tests. For example that, depending on the quarry, the solids feed to the apatite clarifier was about 110 to 140 tons per hour and the solids concentration of the overflow fluctuated between 0.1 and 1%, with the target being that the solids concentration of the overflow is permanently below 0.5%.

Before the tests, a preliminary research of the overflow water characteristics was carried out, in which sedimentation tests, solids concentration and density determination, and particle size analysis were done. In the sedimentation tests is was noticed that there was a little amount of solids that would settle in under a minute, even in a few seconds, giving a settling velocity in the range of 0.03 to 0.003 m/s. Nevertheless, there were also a lot of colloidal solids that would not settle at all, or even some solids that floated.

The solids concentration determination was made according to the SFS-EN 872:2005 standard. The solids concentration of the apatite clarifier overflow samples was of 0.4%. The density of the solution was technically the same as water, which can be explained with the fact that the solids concentration was quite low and did not affect the density of the solution.

Finally, the particle size analysis was made with PAMAS S4031 analyzer, whose measuring range is from 1 to 200 µm. The results of this analysis showed that the larger number of particles was between the size range of 10 to 20 µm or smaller, while the larger volume was given by particles in the size range of 20 to 40 µm.

The tests were held for six days during the last two weeks of July 2015. The pump used in the tests was a Kolmeks ALS 1081/2 pump equipped with a Vacon 20 frequency converter. The maximum head and discharge of the pump, according to the data marked on the pump, were 20 m and 20 l/s respectively and the frequency converter would let to change the discharge for different tests. The SaoxFuge spiral prototype, the pump, and fittings were arranged as shown in Figure 30. The valves at both ends of the system allowed to either return the water to the clarifier or to take the treated water to separated IBC containers.

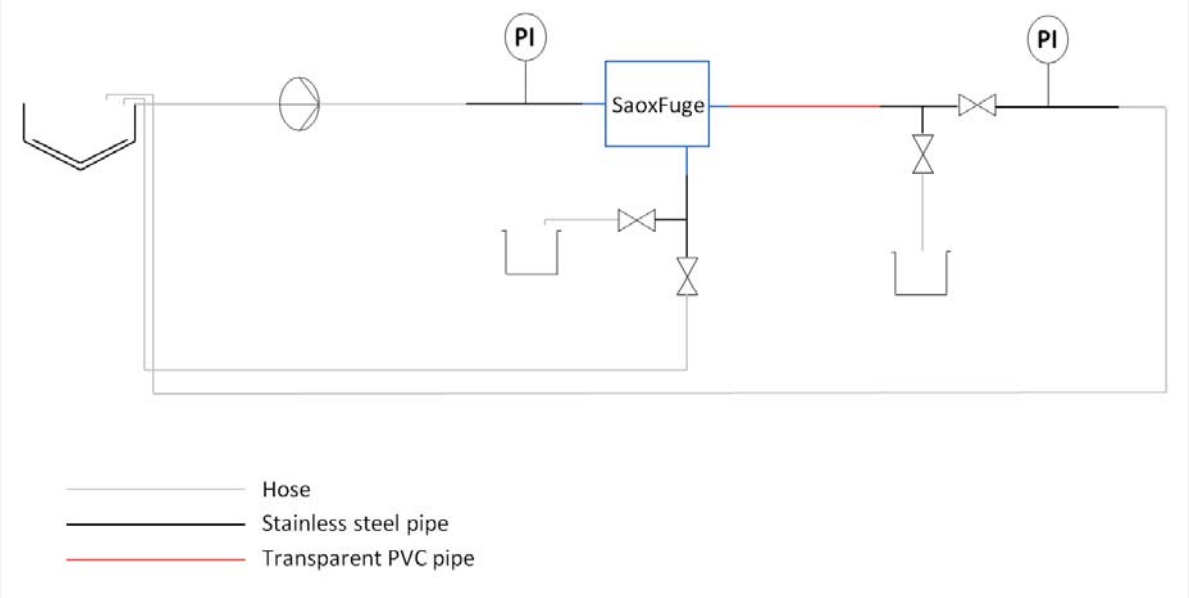

FIGURE 30. SaoxFuge spiral prototype and fittings arrange in the tests (modified from Estrada Reynoso 2015, 17)

The tests were carried out at three different discharges, taking samples both from the IBC containers and from the hoses, returning the exiting main flow to the inflow, and at two different pressures. The pressure was changed by closing almost completely the valve of the main outflow, so that the pressure at the entrance of the device would rise to 1 bar and 2 bar.

The discharge was modified by changing the frequency of the motor of the pump to 25 Hz, 35 Hz, and 45 Hz. Calculating with Equation 29 the resulting discharge at these frequencies, theoretically the discharges would have been 10 l/s, 14 l/s, and 18 l/s respectively. However, measuring the time it took to fill the IBC containers at each frequency, the discharge was slightly lower, being 8 l/s, 12 l/s and 15 - 16 l/s. This difference, although it might result because of the unprecise method of measuring discharge, it might also be due to disturbances generated by the hoses' bends. It could not be tested at the maximum frequency and discharge (50 Hz and 20 l/s), because of insufficient water flow in the channel of the overflow of the clarifier.

For the screw prototype, the test arrangement and testing at different discharges were the same as with the spiral prototype with the difference that, because the device could not be hermetically closed

and there was leakage from the lid, tests were carried out only a couple of times at a frequency of 15 Hz, 25 Hz, and 35 Hz.

Samples of both outflow pipes and of the clarifier overflow were taken during each test. The solids concentration determination and particle size analysis of each sample was made in the laboratory like it was done in the preliminary research.

If there had been solids separation in the prototypes, the solids concentration in the outflow of the smaller pipe would have been greater than the one from the main outflow. However, the results of the tests were inconclusive. While there was a slight difference in a few tests, for example, over double solids concentration in the smaller pipe outflow in one of the tests at a 25 Hz, for other frequencies and in other tests also at 25 Hz there would be very small difference (of about 0.01 to 0.1%) or even a lower solids concentration in the smaller pipe outflow. Also the solids concentration results given by the standard or by the particle analyzer would show differences between them. None of the discharges or test arrangements would clearly indicate solids separation.

There may be a few reasons for these results. The mixing effect of the turbulent flow could be one of the reasons. Nevertheless, since the solids were completely mixed before passing through the device, the solids concentration in both outflows would be the same in every test if the solids continued to be mixed by turbulence. The differences between the solids concentration results between the standard and the particle analyzer are caused by the fact that the standard determines solids concentration by mass, while the particle analyzer determines it by volume. Other reasons would be not enough centrifugal acceleration or retention time to separate the particles, the settling velocities of the particles, or the angle of accumulation not meeting the expansion of the pipe for removal.

Calculating as in Chapter 5 the conditions of the flow at each frequency (with the discharge and head given by Equations 29 and 30), as well as the settling velocities of the particles, it is possible to compare the theoretical conditions of the tests. The results of these calculations are presented in Table 11.

For the calculation of the velocities of the particles, the diameter of the particles was taken as 30 µm, which is the average of the size range that predominated in volume (20 – 40 µm), and their density as the density of apatite, which is of about 3000 kg/m^3 (Geologinen tutkimuslaitos 1982, 18). The shape of the particles is considered spherical, since the particle analyzer results are given according to the characteristics of a spherical particle.

Other things considered in the calculations were that the temperature of the water was 10 °C, and the head loss between the pump and the device was given, in addition to the 90° bends of the device, by the friction loss of the 9 m long lay-flat PVC hose (with a friction loss taken from Kuriyama of America, Inc. 2013, 15) and also by the sudden contractions and expansions caused by the bends of the hose (with a resistance coefficient taken from RIL I 2003, 154).

TABLE 11. Theoretical conditions of the tests at different discharge values

Flow conditions and settling velocities at 25 Hz	
Discharge Q (m^3/s)	0.01
Head (m)	5
Reynolds number	88 294
Velocity of flow v (m/s)	1.05
Total head loss $h_F + h_L$ (m)	1.2
Retention time (s)	5.9
Centrifugal acceleration (m/s^2)	5.91
Magnitude of resultant (m/s^2)	12.46
Angle of direction of resultant (°)	50.37
Discrete particle settling velocity (m/s)	0.0008
Accelerated particle settling velocity (m/s)	0.034
Distance that could be traveled during retention time (m)	0.202
Flow conditions and settling velocities at 35 Hz	
Discharge Q (m^3/s)	0.014
Head (m)	9.8
Reynolds number	123 611
Velocity of flow v (m/s)	1.47
Total head loss $h_F + h_L$ (m)	1.9
Retention time (s)	4.2
Centrifugal acceleration (m/s^2)	11.58
Magnitude of resultant (m/s^2)	16.66
Angle of direction of resultant (°)	35.17
Discrete particle settling velocity (m/s)	0.0008
Accelerated particle settling velocity (m/s)	0.048
Distance that could be traveled during retention time (m)	0.202
Flow conditions and settling velocities at 45 Hz	
Discharge Q (m^3/s)	0.018
Head (m)	16.2
Reynolds number	158 928
Velocity of flow v (m/s)	1.88
Total head loss $h_F + h_L$ (m)	2.9
Retention time (s)	3.3
Centrifugal acceleration (m/s^2)	19.14
Magnitude of resultant (m/s^2)	23.25
Angle of direction of resultant (°)	24.37
Discrete particle settling velocity (m/s)	0.0008
Accelerated particle settling velocity (m/s)	0.062
Distance that could be traveled during retention time (m)	0.202

It is important to mention that the dimensions of the spiral prototype used in the tests are slightly different than the ones pictured in Appendix 1, with a smaller lead angle and with the opening of the separation pipe at 20° below the horizontal centerline of the pipe. Also, the prototype's centerline could not be positioned straightly vertical, so its inclination was of about 12° (Image 1). This inclination was considered in the vector calculations.

IMAGE 1. SaoxFuge spiral prototype position during the tests at Yara's Siilinjärvi site. July 2015

The results of these calculations show that in all cases the direction of the acceleration resultant was towards the area under the opening of the separation pipe, especially in the tests at 25 Hz, where the centrifugal acceleration was smaller than gravity. The distance that could be traveled by the particle during the retention time in the device is in all cases big enough for the particle to arrive to the outer wall of the pipe, which would allow the separation of the particles if located in the separation area.

Also, it is important to notice that the value of this distance is the same for all discharge values. The reason for this is because the distance is calculated by multiplying the retention time by the accelerated particle settling velocity and, since the retention time is inversely proportional to discharge and the settling velocity is directly proportional to discharge, the distance is not affected by changing the discharge value. Thus, the distance that the particle could travel can be affected by changing the particle properties (density, size, shape) or by changing the prototype spiral dimensions.

The particles with the greatest density would arrive to the area defined by the resultant before particles with a lower density but perhaps greater volume. In other words, a particle that has two times the density but the same diameter of another particle will settle faster than a particle that has two

times the diameter but the same density of another particle. If the heavier but smaller particles continued in the main flow due to the resultant's direction and the bigger but lighter particles accumulated in a higher area that could be separated from the main flow, this could explain why in some tests the smaller pipe outflow had higher solids concentration with the particle analyzer and lower concentration with the determination by the standard.

Considering the head given by the pump, even at a frequency of 25 Hz, the head loss due to friction and bends is not that great, theoretically, that it would affect the discharge and explain the difference between the measured and the theoretical discharge.

From all of this it is possible to deduce that, the inconclusive results of the 2015 tests at Yara's Siilinjärvi site might be caused in great part by the insufficient discharge at which the tests were done. This could cause a centrifugal acceleration that is not high enough to overcome the downwards direction of gravity and to accelerate the particles in the direction towards the separation opening of the device. In the future, this can be prevented by choosing a more accurate pump for the tests, as well as by measuring the discharge more precisely with a flow meter located just before the device.

Another reason for the results of the tests might be the particle characteristics of the solids in the solution. Even if the size range of the particles could be known, in the calculations it was assumed that the particles had the density of apatite. However, the particle density was not known and the particles of the overflow of the apatite clarifier could have been of any other material that could be found in the concentration process, perhaps having a lower density than apatite. The characteristics of the particles in the solution would have to be known beforehand so that the theoretical data would be more accurate and the tests of the prototype would be more precise.

Finally, it is appropriate to consider still the probability of mixing due to the turbulent flow and Dean vortices. Some ways to study this are, for example, to have a transparent prototype that would allow observing the areas where mixing and possible vortices occur inside the device, as well as with a deeper theoretical and empirical research with the use of computational fluid dynamics or tomographic analysis of the particles in the device.

7 LABORATORY-SCALE PROTOTYPE DEVELOPMENT

The conclusions made in Chapters 5 and 6 show the need for further testing and development of the SaoxFuge. For a better understanding of the separation efficiency that can be achieved with the SaoxFuge, it is essential to have more control over the variables in the testing of the prototype as well as to identify what are the parameters that affect the separation process the most.

The size of the prototype used in the previous tests required a large discharge and, thus, a large amount of water available to do the testing, which limited the testing location. In other words, the places where the prototype was tested were selected based mainly on their available volume of water and less on the characteristics of the solids in those waters compared to the characteristics of the prototype. Another important factor is the variations in the characteristics of those waters (like solids concentration), which can vary over time and affect also the testing results.

It is because of these reasons that it is suggested testing with a smaller prototype in a laboratory scale. In the laboratory-scale testing the characteristics of the solution to be treated can be more easily known or even artificially made (for example adding a certain amount of particles of known size, density, and shape to water) and, with a smaller prototype, higher centrifugal acceleration can be achieved with a lower discharge. Also sampling of the inflow and both outflows can be more manageable compared to the sampling done from the lay-flat hoses or the IBC containers, and particle size analysis can be achieved inline or online as well.

Based on the calculations made in the previous chapters, an Excel workbook containing the relevant parameters of the calculations was created in order to visualize how each of the parameters affect the results related to the theoretical particle separation. By trying different values of prototype dimensions, particle characteristics, and discharges, it was aimed to find the most suitable ranges of prototype size as well as types of particles for solids separation testing in a certain prototype. Details of this Excel workbook are presented in Appendix 2.

Firstly, for finding these ranges, it was considered that the prototype size has to be changed with respect to the characteristics of the water that has to be treated since the characteristics of the water are particular of each place of origin, so the first step was to gather general data of the particles commonly encountered in water and wastewater treatment facilities. Industrial wastewater was limitedly considered, because the characteristics of the particles in these waters depend on the specific industry from where they come. Besides, the characteristics of the wastewater of a single factory can also vary depending on its production.

According to Tchobanoglous et al. (2014, 1457), the solids in the primary sedimentation sludge have a relative density of about 1.4. For the calculations, also the densities of sand, clay, flocs, and microorganisms were taken from Table 10 in Chapter 3.1.4. The size of the particles was assumed to be between 30 and 1000 µm, which is the size range in which sedimentation is typically considered appropriate. Particles in this size range are, for example, settleable solids, silt particles and some

microbial particles, like bacterial flocs, algae, protozoa, and worms, among others. The density of the settleable solids was taken as 1200 kg/m^3. (Tchobanoglous et al. 2014, 77; RIL II 2003, 106, 508).

Three sizes of prototype were compared to find the minimum density that a spherical particle of certain diameter has to have in order to be separated in each prototype. This was made by considering the distance that the particle could travel during the retention time and assuming there is no mixing due to turbulence or vortices. It is good to notice that, even if both the spiral diameter and the pitch affect the retention time, adding turns to the spiral is more effective for increasing the retention time, so smaller particles have more time to travel to the outer wall of the spiral's pipe.

The dimensions of the biggest prototype were the ones presented in Appendix 1. The sizing of the other prototypes was made by changing the pipe diameter but keeping the relation between the pipe diameter and the dimensions of the spiral somehow similar. The number of turns and the angle of the opening of the separation pipe remained the same for all sizes. Table 12 shows the pipe and spiral dimensions of each prototype used in the calculations as well as the minimum discharge required for the direction of the resultant to be within the opening of the separation pipe.

TABLE 12. Dimensions of the prototypes used in the calculations

Prototype DN100	
Pipe outer diameter (mm)	114,3
Pipe inner diameter (mm)	110,3
Spiral mean diameter (mm)	230
Pitch (mm)	120
Number of turns	5
Lead angle (°)	9,4
Minimum discharge required (m^3/s)	0,020
Prototype DN80	
Pipe outer diameter (mm)	88,9
Pipe inner diameter (mm)	84,9
Spiral mean diameter (mm)	180
Pitch (mm)	95
Number of turns	5
Lead angle (°)	9,5
Minimum discharge required (m^3/s)	0,011
Prototype DN50	
Pipe outer diameter (mm)	60,3
Pipe inner diameter (mm)	56,3
Spiral mean diameter (mm)	122
Pitch (mm)	65
Number of turns	5
Lead angle (°)	9,6
Minimum discharge required (m^3/s)	0,004

The calculations showed that in the particle size range from 30 to 1000 µm the difference of minimum density required for separation between the prototypes is minimal. The minimum value of density for removing a 30 µm particle is about 1250 kg/m^3 for the DN100 prototype, 1200 kg/m^3 for the DN80 prototype, and 1110 kg/m^3 for the DN50 prototype. These densities correspond to the densities of the solids in primary sedimentation sludge and settleable solids, as previously mentioned. The density values increase rapidly and exponentially when the particle size decreases below 10 µm and continue asymptotically close to the value of water density after 100 µm. Figure 31 shows graphically the minimum particle density values in function of particle size for each of the three prototypes.

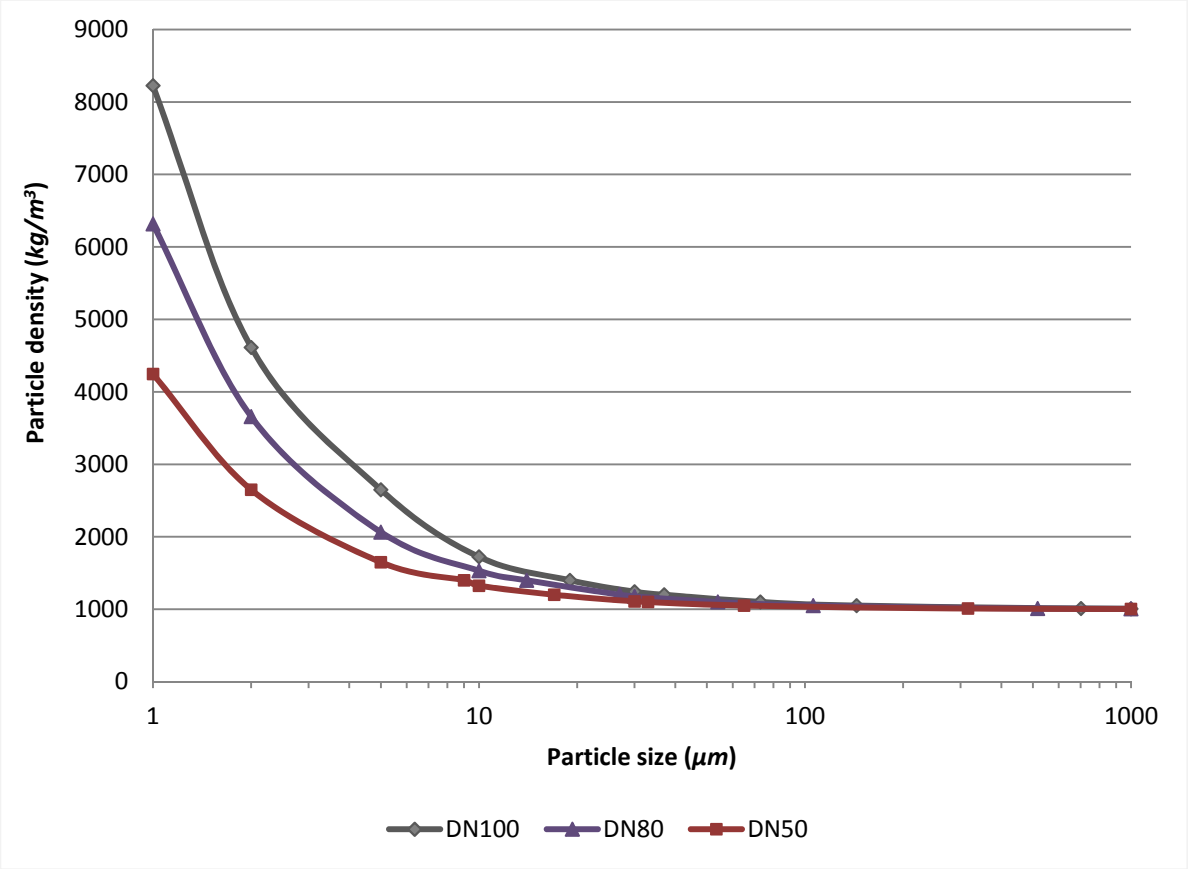

FIGURE 31. Minimum particle density required for separation of particles of a certain size in each prototype

These results show that the DN50 prototype could be a good alternative for the laboratory-scale testing, since between the particle size range for sedimentation there is not a big difference between the bigger and smaller prototypes, and the exponential increase below 10 µm is considerably less steep that than of the bigger prototypes. Also, the discharge required to create a centrifugal acceleration high enough for separation is much lower than that of the DN100 prototype. The DN80 prototype could be an alternative for testing in a pilot-scale between the size ranges for sedimentation, but no for separation of particles whose size is below 10 µm. For these reasons, the following calculations were made only taking into consideration the DN50 prototype.

The density values shown in Figure 31 were calculated assuming that the particles were spherical. Nevertheless, taking into consideration the shape of the particles, the minimum density values of the

different particle sizes were recalculated for the DN50 prototype by modifying the drag coefficient with different sphericity factor values, taken from Table 9 in Chapter 3.1.1. Figure 32 shows graphically the density values in function of particle size at different sphericity factor values.

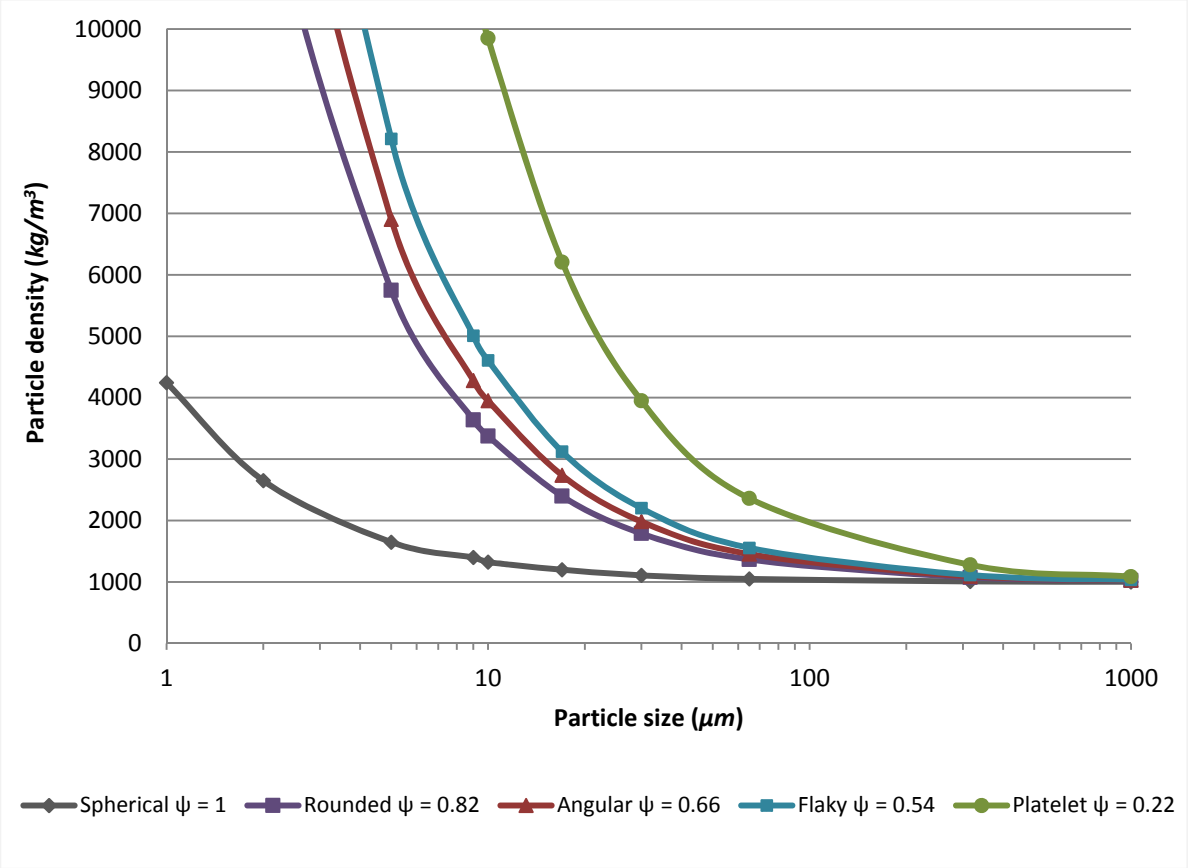

FIGURE 32. Minimum density values for separation of particles of different shapes in the DN50 prototype

The calculations show the effect of particle shape in separation. While for spherical particles in the range from 30 to 1000 µm the minimum density was close to the density of water, for other shapes the minimum density value at 30 µm is almost two times the density of water and it is until a particle size of 200 µm that the density is close to that of water. The exponential growth of the minimum density values of non-spherical particles that are smaller than 30 µm is remarkably steeper than with spherical particles. This would have to be taken into consideration when testing with certain types of water, which is why it is important to do a research of the characteristics of the water to be treated before testing.

Assuming that the laboratory tests of the DN50 prototype will be done using a mixture of sand and silt (with a density of 2650 kg/m^3, a particle size >30 µm, and a sphericity factor of 0.82), the next step is to determine the optimal discharge in the tests. The minimum discharge required for separation presented in Table 12 is the discharge at which the direction of the acceleration resultant is just above the lower end of the separation opening, that is, just below 15°. It is, thus, convenient to increase the centrifugal acceleration and decrease the angle of the resultant as close as possible towards the center of the separation area in order to remove the particles that accumulate under this area as well.

Nevertheless, with an increase in discharge there is also an increase in head losses. Unnecessary large head losses would cause an unnecessary loss of energy. In other words, to overcome the head losses caused by the increase in discharge it would be required a higher pressure head from the pump or a larger difference in elevation head. The total head losses for the DN50 prototype were calculated by considering the friction losses and the minor losses from the 90° bends of the prototype, as well as the friction losses in a pipe between the pump and the prototype.

The length of this pipe has to be long enough so that the flow can stabilize before entering the device. According to the SFS 5059 standard (2007, 3, 12), which gives general instructions for placing instruments, like meters and valves, in the process industry, for some ultrasonic flow meters the minimum distance between a pump and the flow meter is 20 times the diameter of the pipe and the minimum length of straight pipe after the meter has to be at least 5 times the diameter of the pipe. Supposing that there is an ultrasonic flow meter before the DN50 prototype, the minimum distance before the meter would be of about 1.2 m and after the meter about 0.3 m, giving a length of at least 1.5 m of pipe between the pump and the prototype. In the calculations, a pipe length of 2 meters was considered. Figure 33 shows the results of total head loss at different discharge values, as well as the angle of direction of the acceleration resultant at the same discharge values.

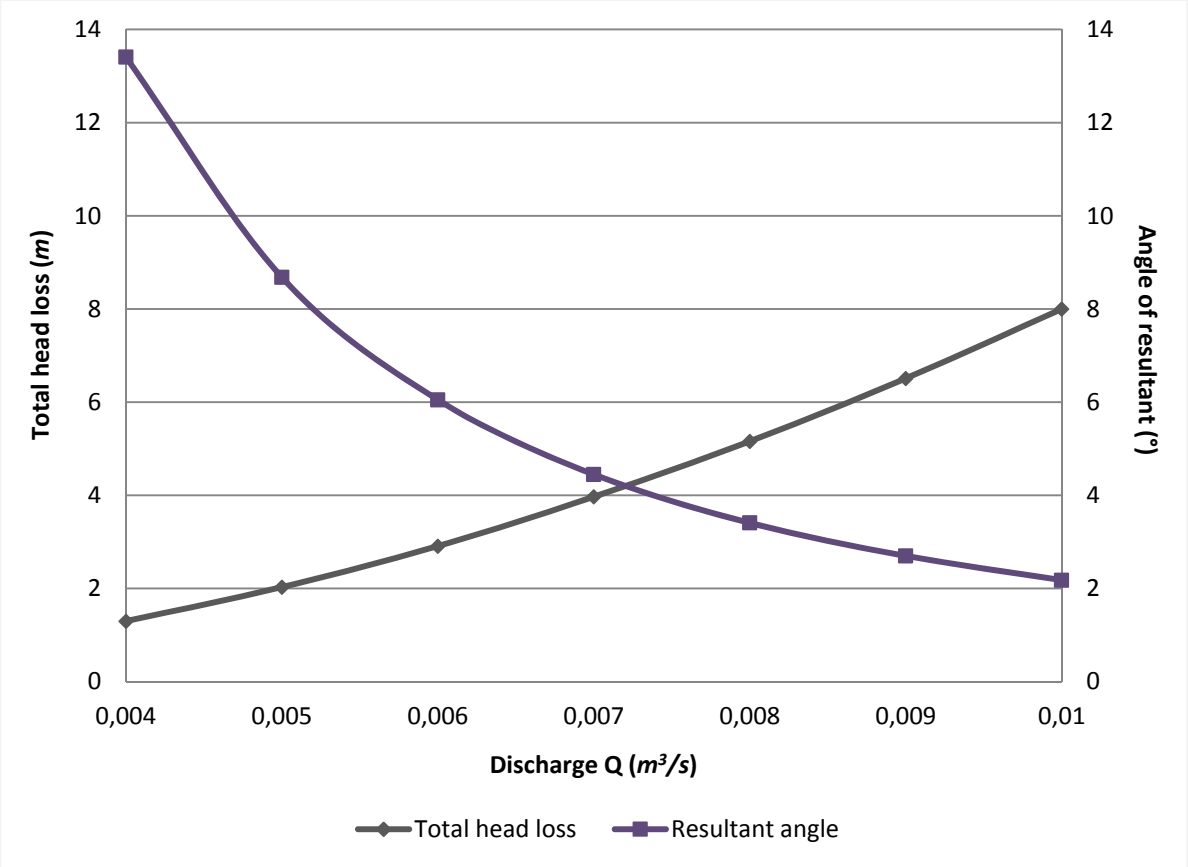

FIGURE 33. Total head loss and angle of resultant at different discharge values

The results of the calculations show that the angle of the resultant decreases rapidly when increasing the discharge. Total head loss, on the other hand, increases steadily while increasing the discharge.

Based on these results, a discharge between 6 and 7 l/s could be appropriate for testing. At this discharge range, the angle of separation is less than half of the one given by the minimum required discharge value and total head loss is only about two meters more.

With this, an appropriate pump for the testing can be chosen, with its highest efficiency between 6 and 7 l/s and a head of at least 5 m. The pump's selection is better done consulting a professional but also the available information provided by manufacturers online is a good aid for this. In this thesis are given some examples of pumps that might be suitable for the testing: the Kolmeks L-50S/4 or the Grundfos DPK.10.50.15.5. Both pumps show a high efficiency between the discharge range of 6 to 7 l/s, and the head given by the pumps is high enough to overcome the head losses calculated previously. The performance curves of these two pumps are presented in Figures 34 and 35.

Besides the discharge and head similarities between both pumps, other similarities are that both have a DN50 outlet and their power requirement at 7 l/s and 12 m is almost the same (about 1.6 kW). Nevertheless, the Kolmeks pump is an inline pump designed to pump clean water, while the Grundfos pump is a submersible pump equipped with a semi-opened impeller with 10 mm free passage that can also be used for pumping drainage. For this reason, between these two pumps, it is the Grundfos pump that is a better option for the laboratory testing of the SaoxFuge DN50 prototype. However, the selection of the pump has to be carefully done before the tests, especially if the characteristics of the water to be treated vary from the assumptions made in this thesis, for example, if the solution is corrosive or there are large particles that could damage the pump's impeller, or if the costs related of the pump are not convenient, among others.

Finally, in addition to the suggestions made in this and the previous chapters, some other considerations for a more controlled laboratory-scale testing can be mentioned. A wider opening of the separation pipe could be considered for increasing the separation possibilities and also for testing at a lower discharge. Making a thoroughly research of the characteristics of the solution and the particles in it, as well as having a flow meter just before the prototype, would give more accurate information about the conditions of the testing, especially for making corrections to the calculations made in this thesis.

Also, settling of the particles before pumping should be avoided. A way to do this is by continuous mixing of the solution in the tank or container from where it is pumped. Last but not least, an accurate method for sampling the outflows is one of the most important aspects to consider, since the results of the tests depend strongly on it. Even if there is a satisfactory solids separation with the prototype, mistakes in sampling can show otherwise, hence, affecting the test results.

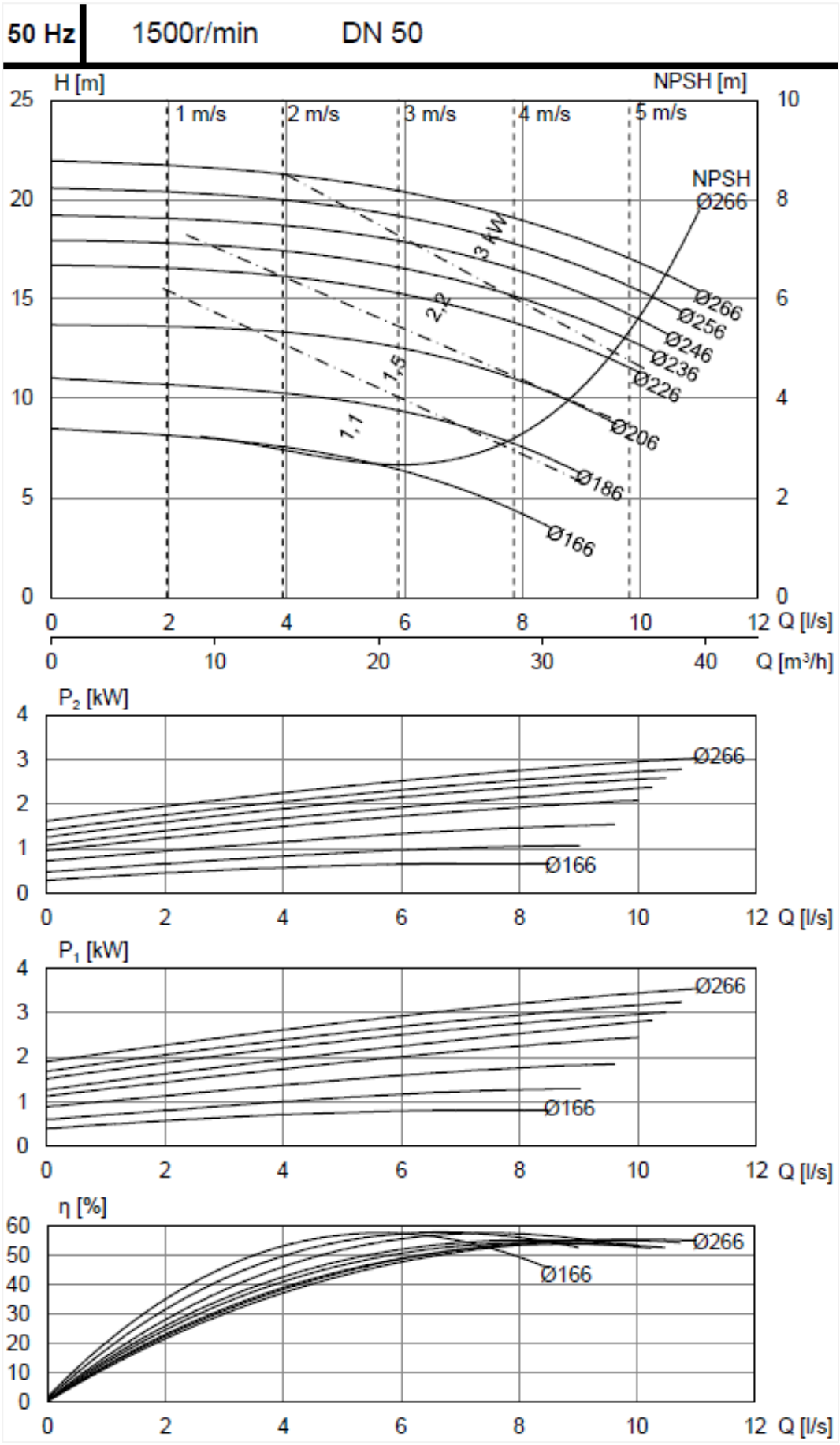

FIGURE 34. Performance curves of the Kolmeks L-50S/4 pump (Kolmeks 2012)

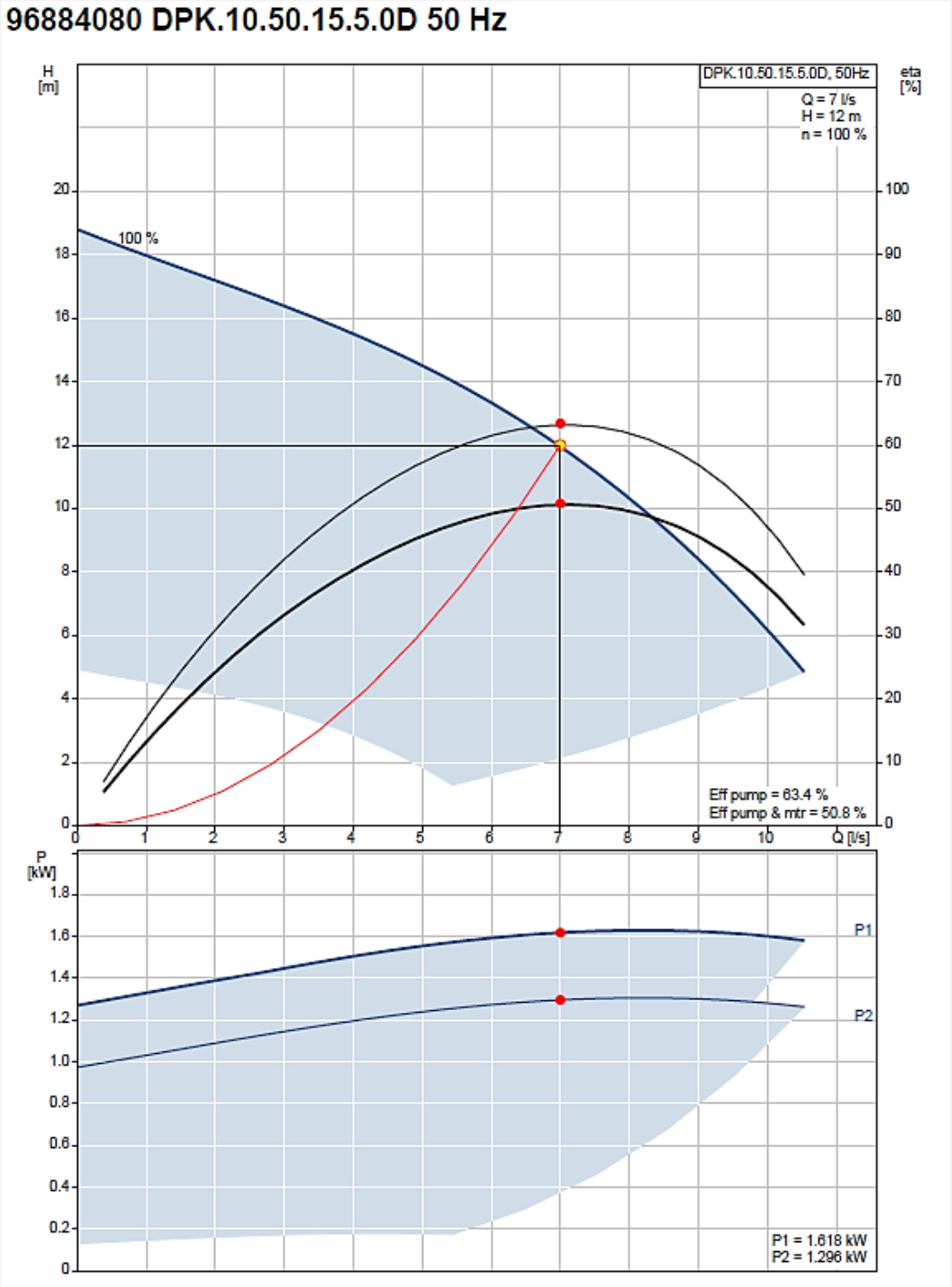

FIGURE 35. Performance curves of the Grundfos DPK.10.50.15.5 pump (Grundfos 2016)

8 CONCLUSIONS

The aim of this thesis was to make a deeper theoretical research of the physical aspects related to solids separation in the SaoxFuge in order to make a review of the previous tests of the pilot-scale prototype and find out the possible causes for the inconclusive results of the tests, as well as to develop a plan for designing and testing a SaoxFuge laboratory-sized prototype for more controlled conditions of testing.

The first part of the thesis was dedicated to the theoretical research. Firstly, in this research, an investigation of the physics and hydraulics linked to particle separation and to pipe flow was carried out. A remarkable realization in this investigation was the theory related to the vortices (known as Dean vortices) generated in curved pipes due to the influence of the centrifugal force. Nevertheless, due to the complexity of the study of these vortices, in the calculations made in the thesis, it was assumed that these vortices do not happen in the SaoxFuge.

The particle separation theory contained basic explanations of the principal characteristics of particles, like size, shape, and density, as well as the basic theory related to particle settling. The latter highlighted the effect of the drag that a particle experiences when moving within a fluid. Also, the way that particles in a certain solution settle has to be determined, in many cases, with sedimentation tests in the laboratory.

In the last part of the theoretical research, the solids separation methods most commonly used in water treatment facilities were described. The purpose of the information gathered in this section was to give some references for comparing the SaoxFuge to these methods. From this, it was noticed that, for example, achieving with the SaoxFuge a centrifugal acceleration that is close to the one achieved by a centrifuge is quite challenging. However, one of the main advantages that the SaoxFuge offers is a retention time much shorter and a needed space much smaller compared to other methods.

In the second part of the thesis, the main conditions of the previous testing of the SaoxFuge prototypes in the summer of 2015 were described and also the plan for the laboratory-sized prototype sizing and testing was developed. The solids separation in the prototype was considered possible if two conditions were met: that a particle traveling in the center of the pipe could travel during the retention time a distance equal or greater than the size of the inner radius of the pipe, and that the direction of the resultant of the acceleration of the particle was towards the opening area of the separation pipe of the prototype.

With the information of the conditions at which the testing of the prototypes was made, it was possible to find possible causes for the inconclusive results of the tests. The calculations made showed that the discharge at which the tests were carried out was not enough to accelerate the particles in a direction towards the area of the opening of the separation pipe, even though the particles could travel a distance much larger than the radius of the pipe during the retention time.

An important observation was that by the distance that the particle could travel during the retention time was not affected by changes in discharge. The reason for this was that even if an increase in discharge would cause the settling velocity of the particle to increase, it would also cause the retention time to decrease in the same proportion. So, changing the prototype dimensions, especially adding turns of the spiral, would be a better way to increase the retention time in order to give a certain particle more time to travel the length of the radius of the pipe.

Lastly, the development of the plan for the laboratory-scale testing was made with the aid of an Excel workbook. All the parameters and formulas used in the calculations related to the solids separation in the SaoxFuge prototype were gathered in this workbook. Warnings are showed in case the angle of the resultant of the acceleration is too big, or if the retention time is too short for the particle to travel the length of the radius of the pipe. In addition to this, information of the pump and fittings before the prototype can be added, and also a warning sign appears if there is risk of pump cavitation. The workbook contains also information about some parameters, like water properties at different temperatures and roughness factors of different pipe materials, as well as diagrams of the sizing parameters of the prototype and a Moody diagram.

The plan for the laboratory-scale prototype considered the characteristics of the solids commonly found in municipal wastewater and the comparison between three different prototype sizes. The results showed that a prototype of size DN50 would be convenient for the testing at a laboratory scale. The optimal particle characteristics for separation with this prototype would be rounded or spherical particles with a size greater than 30 µm and a density between 1100 and 2000 kg/m^3. The calculations also showed that the more the particle shape differs from that of a sphere, the more difficult its separation will be. Flow conditions optimal for this testing would be between 6 and 7 l/s.

The results of this thesis are a general guide for developing a testing plan of the SaoxFuge prototype. The characteristics of the solution to be treated and of the particles in it are the main parameters for the prototype sizing, so it is of main relevance to know this information beforehand. Also a wider opening of the separation pipe or adding turns to the spiral could be considered for increasing the solids separation possibilities of the prototype. When testing the prototype, an adequate sampling method is essential for having trustworthy test results.

In the future, a deeper analysis of the phenomena occurring in the SaoxFuge must be considered. Numerical analysis and computational fluid dynamics would give a better understanding of the flow conditions inside the SaoxFuge and the vortices caused by the spiral shape of the pipe and the turbulent flow. Tomography can also be added to complement the testing of the prototypes. It would help to study how the particles move inside the prototype and to identify critical zones.

REFERENCES

Benjamin, Mark M. & Lawler, Desmond F. 2013. *Water quality engineering: physical/chemical treatment processes*. Hoboken, New Jersey: John Wiley & Sons, Inc.

Benson, Harris. 1995. *University Physics.* Revised edition. New York: John Wiley & Sons, Inc.

Croft, Anthony; Davison, Robert & Hargreaves, Martin. 2001. *Engineering Mathematics: a foundation for electronic, electrical, communications, and systems engineers.* Third edition. Harlow, Essex: Pearson Education Ltd.

Droste, Ronald L. 1997. *Theory and practice of water and wastewater treatment.* New York: John Wiley & Sons, Inc.

Estrada Reynoso, Priscila. 2015. *Kiintoaineenerotuslaitteen SaoxFugen tutkimus. KaivosVV -hanke, Yara Suomi Oy:n Siilinjärven rikastamo.* [Electronic report] Located in the author's electronic files.

Forsythe, William Elmer. 1954; 2003. *Smithsonian physical tables.* Ninth edition. Norwich, New York: Knovel. [Accessed on 16 February 2016] Available from: https://app.knovel.com/web/view/swf/show.v/rcid:kpSPTRE008/cid:kt002VRH31/viewerType:pdf/root_slug:smithsonian-physical?cid=kt002VRH31&page=16&q=effect%20of%20pressure%20upon%20viscosity&b-q=effect%20of%20pressure%20upon%20viscosity&sort_on=default&b-subs

Geologinen tutkimuslaitos. 1982. *Perustietoa malminetsijälle. Opas 9.* [Web document] Espoo: Geologinen tutkimuslaitos. [Accessed on 31 March 2016] Available from: http://tupa.gtk.fi/julkaisu/opas/op_009.pdf

Graebel, W. P. 2001. *Engineering fluid mechanics.* New York: Taylor & Francis Publishers.

Grundfos Pumps Corporation. 2016. *Grundfos Product center. Find product.* [Accessed on 15 April 2016] Available from: http://product-selection.grundfos.com/product-detail.product-detail.html?custid=GMA&productnumber=96884080&qcid=86311525

Hamill, Les. 2011. *Understanding Hydraulics*. Third edition. Basingstoke, Hampshire: Palgrave Macmillan.

Holdich, Richard G. 2002. *Fundamentals of particle technology*. Shepshed, Leicestershire: Midland Information Technology and Publishing. [Accessed on 19 February 2016] Available from: http://particles.org.uk/particle_technology_book/particle_book.htm

Karassik, Igor J; Messina, Joseph P.; Cooper, Paul & Heald, Charles C. 2001. *Pump Handbook*. Third edition. New York: McGraw-Hill.

Keränen, Mikko. 2015. Mill manager at Yara Finland Siilinjärvi site. [Email] Receivers Priscila Estrada Reynoso, Eero Antikainen and Pasi Pajula. Sent on 5 June 2015.

Knight, Randall D. 2014. *Physics for Scientists and Engineers: a strategic approach with modern physics.* Third edition. Harlow, Essex: Pearson Education Ltd.

Kolmeks Oy. 2012. *Materiaalipankki. Datalehdet. Keskipakopumput. L_-50S/4*. [Accessed on 15 April 2016]. Available from: http://www.kolmeks.fi/materiaalipankki/datalehdet/keskipakopumput

Kundu, Pijush K.; Cohen, Ira M. & Dowling, David R. 2012. *Fluid Mechanics*. Fifth edition. Oxford: Elsevier Inc.

Kuriyama of America, Inc. 2013. *Layflat discharge hoses*. [Web catalogue]. Schaumburg, Illinois: Kuriyama of America, Inc. [Accessed on 31 March 2016] Available from: http://products.kuriyama.com/asset/Kuriyama-Layflat-Products-16-Pg--Catalog_LR_-Final-3-01-13GK.pdf

Mezger, Thomas G. 2006. *The rheology handbook: for users of rotational and oscillatory rheometers.* Second revised edition. Hannover: Vincentz Network GmbH & Co. [Accessed on 3 February 2016]. Available from: https://books.google.fi/books?id=N9Fdn0MEI-DIC&pg=PA29&hl=fi&source=gbs_toc_r&cad=3#v=onepage&q&f=false

Peker, Sümer M. & Helvaci, Şerife Ş. 2008. *Solid-liquid two phase flow.* Amsterdam, NL: Elsevier. [Accessed on 19 February 2016] Available from: https://app.knovel.com/web/view/pdf/show.v/rcid:kpSLTPF001/cid:kt00C50672/viewerType:pdf/root_slug:solid-liquid-two-phase/url_slug:classification-separation?cid=kt00C50672&b-q=hydrocyclone&b-subscription=TRUE&b-group-by=true&b-search-type=tech-reference&b

RIL. 2003. *124-1 Vesihuolto I.* Helsinki: Suomen Rakennusinsinöörien Liitto RIL r.y.

RIL. 2003. *124-1 Vesihuolto II.* Helsinki: Suomen Rakennusinsinöörien Liitto RIL r.y.

SansOx. 2015. *SansOx Solutions 2015*. [Power Point presentation] Helsinki. Received via email from Juhani Pylkkänen on 3 November 2015.

SansOx. 2016. [Website] [Accessed on 13 April 2016] Available from: www.sansox.fi

SFS 5059. 2007. *Instrumentation. Placing of Process Instruments*. Second Edition. Helsinki: Finnish Standards Association.

Tchobanoglous, George; Stensel, H. David; Tsuchihashi, Ryujiro; Burton, Franklin; Abu-Orf, Mohammad; Bowden, Gregory & Pfrang, William. 2014. *Wastewater engineering: treatment and resource recovery*. Fifth edition. New York: McGraw-Hill Education.

Tuomenlehto, Ari; Holmlund, Eero; Huuskonen, Maija; Makkonen, Heikki & Surakka, Jarkko. 2014. *Insinöörin matematiikka.* First edition. Helsinki: Edita.

United Nations Committee on Economic, Social, and Cultural Rights. 2002. *General Comment No. 15. The right to water (arts. 11 and 12 of the International Covenant on Economic, Social and Cultural Rights)*. Geneva. [Accessed on 13 April 2016]. Available from: https://documents-dds-ny.un.org/doc/UNDOC/GEN/G03/402/29/PDF/G0340229.pdf?OpenElement

World Health Organization (WHO). 2015. *Media centre. Fact sheets. Drinking water*. [Website] June 2015. [Accessed on 28 January 2016] Available from: http://www.who.int/mediacentre/factsheets/fs391/en/

CONFIDENTIAL

APPENDIX 2. EXCEL WORKBOOK TOOL

An Excel workbook containing the parameters, formulas, and general data used in this thesis for the calculation of the theoretical particle separation in the SaoxFuge was developed as a tool for a quick analysis of how different parameters in the design of the prototype and the test conditions affect the particle separation.

The workbook contains two worksheets, one containing the data and the calculations and another one containing information for obtaining certain parameters. The Tables and diagrams worksheet contains tables with values for water density, viscosity, and vapor pressure, pipe DN sizes and roughness factors, resistance coefficients, and sphericity factors as well as a diagram of the prototype dimensions and a Moody diagram.

The calculations in the Data worksheet are separated into four subjects: prototype characteristics and dimensions, flow characteristics, particle characteristics, and pump and fittings. The cells containing formulas are white-colored, while the cells containing variables are colored in four different colors (green, blue, violet and red) depending on the type of parameter they contain. The variables in the prototype design are green-colored cells, values taken from tables are blue-colored cells, values taken from diagrams are violet-colored cells, and test variables are red-colored cells. Next, the contents of each of these tables will be explained.

Prototype characteristics and dimensions

In the Prototype characteristics and dimensions table, those parameters related to the prototype pipe size, material, and roughness factor as well as the parameters related to the spiral dimensions and mounting angle are given. With these parameters, the length of the pipe as well as the lead angle are calculated according to Equations A and B. Diagrams showing the location of these parameters, the outer diameters in millimeters and inches of DN pipes, and a table with the roughness factors of some common pipe materials are given in the Tables and diagrams worksheet. Figure A shows the Prototype characteristics and dimensions table, Figure B and C show the diagrams of the prototype design parameters.

$$l_p = n\sqrt{p^2 + \left(\pi * \frac{D}{2}\right)^2} + L \qquad \text{(Eq. A)}$$

$$\theta = tan^{-1}\left(\frac{p}{\pi * D}\right) \qquad \text{(Eq. B)}$$

where l_p is the length of pipe, n is the number of turns, D is the spiral mean diameter, L is the length of straight pipe before the first turn in the spiral, and θ is the lead angle of the spiral.

Prototype characteristics and dimensions	
Pipe	
Outer diameter (mm)	114,3
Inner diameter (mm)	110,3
Length (m)	3,86
Material	Stainless steel, welded
Roughness factor *k* (mm)	0,1
Spiral	
Mean diameter (mm)	230
Pitch (mm)	120
Turns	5
Length of straight pipe (mm)	200
Opening angle of separation pipe (°)	15
Lead angle (°)	9,4
Mounting angle (°)	0

FIGURE A. Prototype characteristics and dimensions table

FIGURE B. Pipe and spiral dimensions diagram

FIGURE C. Lead angle of spiral and angle of the opening of the separation pipe

Flow characteristics

In the Flow characteristics table are the values related to the hydraulics of the flow and the centrifugal acceleration and resultant values. There are three main sections: properties of the fluid, hydraulics and physics (Figure D). The values for properties of the fluid, usually water, depend on its temperature and, based on it, the values for density, viscosity, and vapor pressure of the water can be taken from a table in the Tables and diagrams worksheet. The atmospheric pressure and vapor pressure of water are relevant to determine if there is a risk of pump cavitation in the Pump and fittings table. The pressure head is calculated by subtracting the total head losses to the head given by the pump.

In the hydraulics section, the values for discharge and friction factor are introduced for calculations of the flow velocity, Reynold's number, friction losses, minor losses, total head losses and retention time. All of these are calculated as presented in Chapter 5 in this thesis. Minor losses are calculated in the Pump and fittings table. The volume taken in the calculation of the retention time is calculated by multiplying the cross-sectional area of the pipe times its length. The friction factor can be determined from the Moody diagram in the Tables and diagrams worksheet.

In the physics section, the gravitational and centrifugal acceleration as well as the magnitude and angle of direction of the acceleration resultant are presented. The flow velocity and the spiral's mean diameter are taken for the centrifugal acceleration calculation as shown in Chapter 5. The calculation of the magnitude and angle of direction of the resultant is done according to Equations C and D.

$$a_r = \sqrt{{a_g}^2 + {a_c}^2 - 2\, a_g\, a_c\, cos(180 - (90 - \beta))} \qquad \text{(Eq. C)}$$

$$\gamma = cos^{-1}\left(\frac{{a_g}^2 - {a_r}^2 - {a_c}^2}{2\, a_r\, a_c}\right) \qquad \text{(Eq. D)}$$

where a_r is the resultant acceleration, a_g is the gravitational acceleration, a_c is the centrifugal acceleration, β is the mounting angle and γ is the angle of direction of the resultant.

If the angle of the resultant is greater than the angle of the opening of the pipe, a warning appears next to it, as shown in Figure E.

Flow characteristics	
Fluid (water)	
Temperature (°C)	4
Density (kg/m^3)	1000
Dynamic viscosity μ (Ns/m^2)	1,352E-03
Vapor pressure (kN/m^2)	0,87
Atmospheric pressure (kN/m^2)	101,325
Pressure head (m)	8,71
Hydraulics	
Velocity v (m/s)	2,093
Discharge Q (m^3/s)	0,02
Reynolds number	1,71E+05
Friction factor (D-W)	0,021
Friction head loss h_F (m)	0,16
Minor losses h_L (m)	3,13
Total head loss (m)	3,29
Retention time (s)	1,85
Physics	
Gravitational acceleration (m/s^2)	9,81
Centrifugal acceleration (m/s^2)	37,07
Centrifugal acceleration (G)	3,8
Magnitude of resultant (m/s^2)	38,35
Angle of resultant (°)	14,82

FIGURE D. Flow characteristics table

Magnitude of resultant (m/s^2)	13,50	
Angle of resultant (°)	46,63	**Under opening!**

FIGURE E. Warning shown when the angle of direction of the acceleration resultant is too big

Particle characteristics

Values of particle size and density are introduced in the Particle characteristics table (Figure F). With this data is calculated the particle cross-sectional area and volume. The particle sphericity factor is taken from a table in the Tables and diagrams worksheet. If the factor equals to 1, the drag coefficient value is set to be 0.4. If a different sphericity factor is introduced, the drag coefficient is calculated as in Chapter 5.

The results are used for calculation of the discrete settling velocity and accelerated settling velocity of the particle, as well as the calculation of the distance that could be traveled by the particle during the retention time. The formulas used are the ones used for these calculations in Chapter 5. If the distance that could be traveled value is less than the inner radius of the prototype's pipe, a warning appears (Figure G).

Particle characteristics	
Particle	
Diameter (μm)	30
Density (kg/m^3)	2000
Cross-sectional area (m^2)	7,07E-10
Volume (m^3)	1,41E-14
Sphericity ψ	1
Drag coefficient C_D	0,4
Discrete settling velocity (m/s)	0,0004
Accelerated settling velocity (m/s)	0,0609
Distance traveled during retention time (m)	0,1124

FIGURE F. Particle characteristics table

Accelerated settling velocity (m/s)	0,0193	
Distance traveled during retention time (m)	0,0355	**Not enough time**

FIGURE G. Warning shown when the distance that could be traveled during retention time is too short

Pump and fittings

Finally, in the Pump and fittings table (Figure H) the values of head and discharge of the pump used in the test can be introduced. If the pump is not a submersible pump, the NPSH, suction lift and friction head loss of the suction pipe can be introduced for determining if there is pump cavitation risk. If there is no cavitation risk, a message that reads "OK" appears next to the NPSH value. If there is cavitation risk, a warning will appear (Figure I).

The minor losses caused by fittings before the prototype and the friction loss in the pipe between the pump and the prototype are calculated in the fittings section. In this section, a description of the type of fitting, its resistance coefficient, and its number or length are introduced in order to calculate the minor losses. Resistance coefficients of some fittings are given in the Tables and diagrams worksheet.

Pump and fittings

Pump

Discharge Q (m^3/s)	0,007	
Head (m)	12	
NPSH	0	OK
Suction lift (m)	0	
h_F in suction pipe (m)	0	

Fittings

Type	*K*	*Number*	*Loss (m)*	*Total loss*
90° bend, r/D = 1	0,4	20	1,05	
Sudden contraction	0,45	3	0,18	
Sudden expansion	0,75	3	0,30	
			0,00	
Type	*m/m*	*Length*	*Loss (m)*	
Layflat PVC hose	0,06	9	0,54	
			0,00	
			0,00	
			0,00	
Length of pipe after pump		2	0,12	
				2,19

FIGURE H. Pump and fittings table

Pump		
Discharge Q (m^3/s)	0,007	
Head (m)	12	
NPSH	5	Cavitation risk!
Suction lift (m)	5	
h_F in suction pipe (m)	5	

FIGURE I. Pump cavitation risk warning